SYSTEMATIC INVESTIGATION OF HYDROGEL MATERIAL PROPERTIES ON CELL RESPONSES FOR VOCAL FOLD AND VASCULAR GRAFT TISSUE ENGINEERING

A Dissertation

by

ALLEN BULICK

Submitted to the Office of Graduate Studies of
Texas A&M University
in partial fulfillment of the requirements for the degree of

DOCTOR OF PHILOSOPHY

August 2009

Major Subject: Chemical Engineering

SYSTEMATIC INVESTIGATION OF HYDROGEL MATERIAL PROPERTIES ON CELL RESPONSES FOR VOCAL FOLD AND VASCULAR GRAFT TISSUE ENGINEERING

A Dissertation

by

ALLEN BULICK

Submitted to the Office of Graduate Studies of
Texas A&M University
in partial fulfillment of the requirements for the degree of

DOCTOR OF PHILOSOPHY

Approved by:

Chair of Committee:	Mariah S. Hahn
Committee Members:	Michael Pishko
	Zhengdong Cheng
	Melissa Grunlan
Department Head:	Michael Pishko

August 2009

Major Subject: Chemical Engineering

ABSTRACT

Systematic Investigation of Hydrogel Material Properties on Cell Responses for Vocal Fold and Vascular Graft Tissue Engineering. (August 2009)

Allen Bulick, B.S., Texas A&M University

Chair of Advisory Committee: Dr. Mariah Hahn

The research presented here deals with synthetic materials for application in tissue engineering, primarily poly(ethylene glycol) (PEG) and poly(dimethyl siloxane)$_{star}$ (PDMS)$_{star}$. Tissue engineering seeks to repair or replace damaged tissue through implantation of cell encapsulated in an artificial scaffold. Cell differentiation and extracellular matrix (ECM) deposition can be influenced through a wide variety of *in vitro* culture techniques including biochemical stimuli, cell-cell interactions, mechanical conditioning and scaffold physical properties. In order to systematically optimize *in vitro* conditions for tissue engineering experiments, the individual effects of these different components must be studied. PEG hydrogels are a suitable scaffold for this because of their biocompatibility and biological "blank slate" nature.

This dissertation presents data investigating: the effects of glycosaminoglycans (GAGs) as biochemical stimuli on pig vocal fold fibroblasts (PVFfs); the effects of mechanical conditioning and cell-cell interactions on smooth muscle cells (SMCs); and the effects of scaffold physical properties on SMCs. Results show that GAGs influence PVFf behavior and are an important component in scaffold design. Hyaluronic acid

(HA) formulations showed similar production in collagen I and III as well as reduced levels of smooth muscle α-actin (SMα-actin), while chondroitin sulfate (CSC) and heparin sulfate showed enriched collagen III environments with enhanced expression of SMα-actin.

A physiological flow system was developed to give comprehensive control over *in vitro* mechanical conditioning on TEVGs. Experiments performed on SMCs involved creating multi-layered TEVGs to mimic natural vascular tissue. Constructs subjected to mechanical conditioning with an endothelial cell (EC) layer showed enhanced expression of SMC differentiation markers calponin h1 and myocardin and enhanced deposition of elastin. Consistent with other studies, EC presence diminished overall collagen production and collagen I, specifically.

Novel $PDMS_{star}$-PEG hydrogels were studied to investigate the effects of inorganic content on mesenchymal stem cell differentiation for use in TEVGs. Results agree with previous observations showing that a ratio of 5:95 $PDMS_{star}$: PEG by weight enhances SMC differentiation markers; however, statistically significant conclusions could not be made. By studying and optimizing *in vitro* culture conditions including scaffold properties, mechanical conditioning and multi-layered cell-cell interactions, TEVGs can be designed to maximize SMC differentiation and ECM production.

ACKNOWLEDGEMENTS

I would like to thank Dr. Mariah Hahn for her support and guidance through my PhD research and learning experience. She has been an excellent mentor and teacher, allowing me exposure to many different research areas within tissue engineering and letting me work on experiments that stimulated my interest in this area. Research was challenging and required the mastery of new skills and problem solving techniques and allowed me to address challenges both independently and in a group setting.

I would also like to thank my committee members, Dr. Michael Pishko, Dr. James Silas, Dr. Zhengdong Cheng and Dr. Melissa Grunlan for their time and effort. A special thanks to Dr. Melissa Grunlan for her collaborative contributions to this work.

Also, my group members from the Hahn research group contributed significantly to my research and helped me learn new techniques and complete successful experiments. This research would not have been possible without group contributions. I would also like to thank members from the Grunlan (Biomedical Engineering) research group for development and characterization of the $PDMS_{star}$ materials and for their help in the experiment covered in Chapter VII.

TABLE OF CONTENTS

Page

CHAPTER Page

CHAPTER Page

LIST OF FIGURES

FIGURE Page

FIGURE Page

LIST OF TABLES

CHAPTER I

INTRODUCTION

1.1 Overview

Tissue engineering is a constantly expanding and developing field. Currently, there exist a multitude of treatments with both natural and synthetic materials. The research presented here deals with synthetic materials for application in tissue engineering, primarily poly(ethylene glycol) (PEG) and poly(dimethyl siloxane)$_{star}$ (PDMS)$_{star}$. The typical modern definition of tissue engineering can be attributed to Langer and Vacanti, where they stated that tissue engineering is "an interdisciplinary field that applies the principles of engineering and the life sciences toward the development of biological substitutes that restore, maintain or improve tissue function (*1*)." Typically, tissue engineering is conducted by creating a scaffold with requisite mechanical properties, implanting cells into that scaffold, and using it to replace damaged tissue. Some treatments without cell encapsulation that rely on the migration of native cells into the artificial scaffold have also been developed (*2-4*). Many of the earliest successes in tissue engineering were related to skin grafts, but recent advances have broadened the impact to areas such as cartilage regeneration, bone regeneration and vascular grafts (*5-7*).

This dissertation follows the style of *Science*.

From whichever material the scaffold is created, it must provide the bulk of the mechanical strength of the replaced tissue until the cells have created enough natural extracellular matrix (ECM) to replace the synthetic scaffold (*8*). Synthetic materials are generally more flexible and yield greater control over their mechanical properties than their natural counterparts (*8*). There are many ways to achieve the desired physical properties, and scaffolds come in a variety of forms including hydrogels, porous blocks, fibrous bundles, or custom shapes. Most of the forms are achieved through some type of crosslinking. Several crosslinking methods exist including chemical, physical and biological (*9-15*). The research presented here utilizes chemical crosslinking to generate hydrogel scaffolds. Figure 1.1 illustrates the different forms of the synthetic scaffolds (*8*).

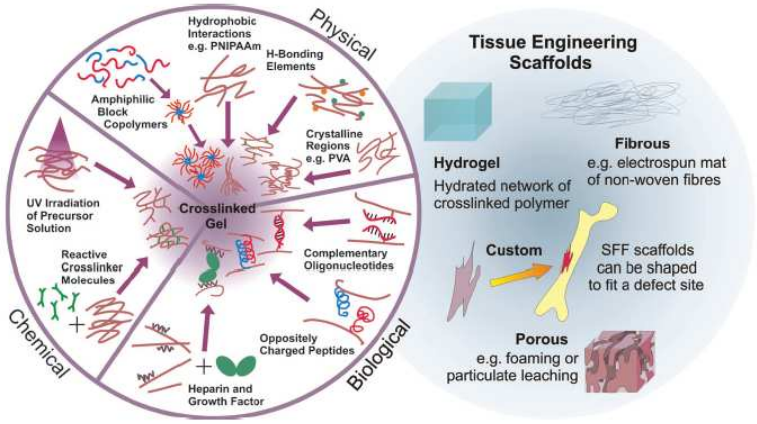

Figure 1.1: Crosslinking mechanisms and scaffold forms in tissue engineering (*8*)

Utilizing the PEG and $PDMS_{star}$-PEG co-hydrogels, this research will focus on two areas of tissue engineering; namely, vocal fold regeneration and tissue engineered vascular grafts (TEVGs). Several methods will be employed to explore the various

components that have been found to influence cell behavior. Specifically, these include: biochemical stimuli, mechanical conditioning, cell-cell interactions and scaffold physical properties.

1.2 Vocal Folds

1.2.1 Motivation

The vocal folds are a unique tissue in relation to both the frequency (100-1000Hz) and amplitude (~1mm or 30% strain) of vibrations, causing accelerations of 200-300g. Voice production is heavily dependent on the biomechanical properties of the surrounding tissue and ECM (*16, 17*). As a laminated structure, it is composed primarily of a stratified squamos epithelium, lamina propria and a thyroarytenoid muscle. In phonation, the lamina propria, or connective tissue layer, exhibits a significant effect due to its viscoelastic properties. The lamina propria is primarily composed of fibrous proteins, e.g. elastin and collagen, and various interstitial proteins such as glycosaminoglycans (GAGs), e.g. hyaluronic acid (HA) and heparin sulfate (HS). These proteins are important contributors to biomechanics controlling strength, elasticity and viscosity (*16-18*). Figure 1.2 shows a diagram of the typical vocal fold structure (*17*).

Damage to the superficial lamina propria (SLP) can be caused be a multitude of factors such as laryngeal cancer and excessive voice strain leading to problems manifested in ways such as nodules, polyps and other deformities. Upon healing, the

SLP is left scarred which can affect the ability for phonation by changing the biomechanical properties of the remaining tissue. Various speech and voice disorders of this nature have been shown to affect ~3-5% of the population, and there is yet a suitable method for repairing the damaged (*16-18*). Methods currently in use include physical therapy and surgery by implantation of synthetic or natural ECMs such as collagen and Teflon (*19-23*).

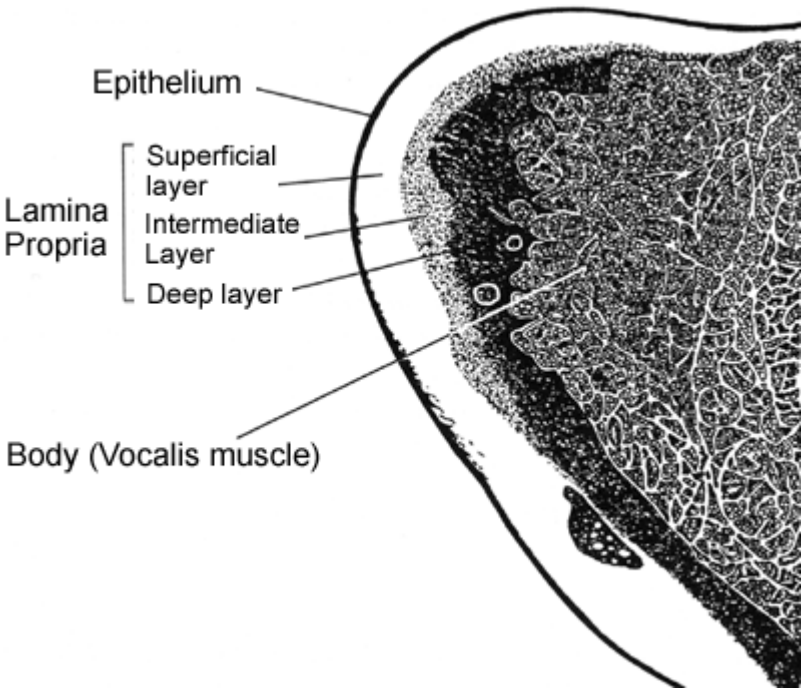

Figure 1.2: Structure and makeup of vocal fold tissue (*17*)

1.2.2 Research

Tissue engineering now has a role in creating new materials for implantation to assist in repair to the damaged and scarred areas of the lamina propria. Tissue

engineering methods under study range from natural ECMs (collagen, HA and derivatives) to synthetic (poly(lactic acid) (PLA), poly(glycolic acid) (PLG), PEG as well as xenogenic (porcine)). Together, the SLP and surrounding epithelium comprise the mucosa whose altered viscoelastic properties lead to the many voice disorders. Vocal fold tissue has three main cellular components, namely: myofibroblasts, microphages and fibroblasts. The vocal fold fibroblasts maintain the lamina propria and participate in the replacement and manufacture of new fibrous and interstitial proteins (*18-20, 22, 24*).

PEG is an attractive choice among the synthetic ECMs in that its non-biofouling properties render it a "blank slate" material, facilitating the study of cellular response without effects from the environment (*25*). It can also be modified to allow for photocrosslinking (PEG diacrylate (DA)) and to include biochemically active proteins such as GAGs and proteoglycans (*26-28*). An example of this is included in Figure 1.3 (*28*). In order to engineer materials for vocal fold repair, cellular response in a synthetic ECM must be optimized. This can be done by individually studying the various effects of components from natural vocal fold tissue on cellular production and response. The work presented here concerns *in vitro* 3D culture of pig vocal fold fibroblasts (PVFf) in PEGDA with four GAGs found to participate in vocal fold tissue. The four GAGs chosen include the widely studied HA, as well as HS, dermatan sulfate (DS) and chondroitin sulfate C (CSC) (*22, 29-32*). PVFf were encapsulated with one of the specified GAGs and cultured *in vivo* for a period of 2.5 weeks. After sample collection, the cells were characterized quantitatively and qualitatively for ECM deposition of

elastin, collagen type I and III. DNA was also measured as a means to determine cell viability through culture.

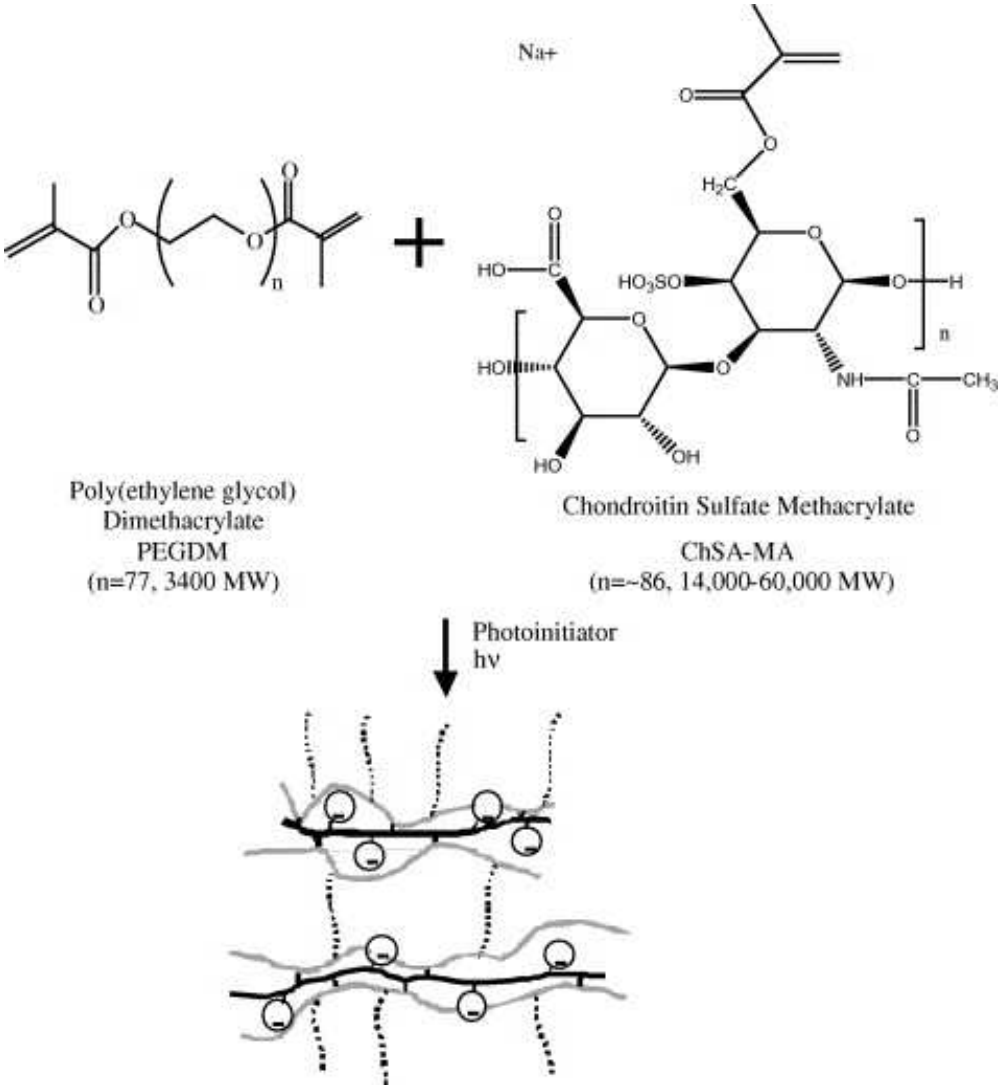

Figure 1.3: Reaction scheme for a PEG hydrogel functionalized with CSC (*28*)

1.3 Tissue Engineered Vascular Grafts

1.3.1 Motivation

Cardiovascular disease is the leading cause of fatalities world wide across every demographic. Arterial bypass surgeries are commonplace and one of the main methods of alleviating atherosclerosis and other conditions. Approximately 500,000 of these procedures are performed in the US annually (*33*). The synthetic materials Dacron and Teflon have been successfully used in large diameter arterial replacement applications. However, due to several issues, these materials, as well as attempts with other methods, have met with little success when dealing with small diameter (<6mm) vasculature (*34*). The main reasons for TEVG failure in the past have been one or a combination of: thrombosis due to lack of a compatible endothelium, restenosis due to inflammatory response and infection and mechanical failure due to lack of sufficient strength. Synthetic materials have high occlusion at lower diameters and attempts for implantation of TEVGs made from natural sources, such as collagen, have experienced problems maintaining sufficient tensile strength *in vivo* (*35-37*).

Successful TEVGs must address the shortcomings of past attempts. Namely, they must be able to withstand the shear and cyclic stresses experienced *in vivo* and abstain from inducing an inflammatory response. This has led to the development of TEVGs *in vitro* in an attempt to prepare them for *in vivo* implantation (*6*). Most work has focused on the medial layer of vascular tissue, composed and maintained by smooth

muscle cells (SMCs) (*38-41*). In order to develop functional TEVGs suitable for use *in vivo,* the SMCs must be conditioned in such a way so that they may produce their own ECM to replace the damaged vascular tissue in the body. By accomplishing this, TEVGs may address some limitations of natural source grafts that did not have sufficient mechanical properties similar to that of the native vascular tissue. The SMC layer is buttressed by an inner endothelial layer and an outer adventitial layer, composed of fibroblasts. A cross-section of a blood vessel showing the multi-layered architecture is shown in Figure 1.4 (*42*).

Investigations into the variables affecting medial layer development have independently confirmed the importance of a wide variety of components. These variables can be arranged into two subgroups. Group 1 consists of the scaffold in which the cells are seeded; specifically its biochemical, mechanical and morphological properties. Group 2 consists of *in vitro* development conditions, i.e. mechanical conditioning and cell-cell interactions. Studies of multi-cell layered constructs under mechanical conditioning *in vitro* have been limited. This is an important subsequent step in the development of these grafts as cell-cell interactions may differ in the presence of conditioning. The long-term desire of TEVGs is to have the artificial scaffold degrade as it is replaced by the natural ECM of the encapsulated cells. Initially, however, the synthetic scaffold has a large influence on cell activity; therefore, optimizing its properties such as mesh size and elastic modulus are important. The central hypothesis of this work is that we can modulate SMC behavior, differentiation and ECM production by optimizing its *in vitro* culture conditions.

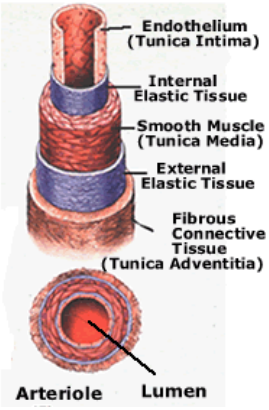

Figure 1.4: Structure of a blood vessel (*42*)

1.3.2 Research

The goal of this research is to elucidate and optimize the combinatorial effects of scaffold properties and *in vitro* culture conditions on SMC ECM production and differentiation. Specifically, we will investigate:

- Material properties including inorganic content and elastic modulus
- Effects of mechanical conditioning and cell-cell interactions

Development of technology in this area benefits from a large patient base as well as the potential to save lives. Variables from group 2 consist of mechanical conditioning and cell-cell interactions. *In vivo*, cells experience both cyclic tensile strain and transmural shear stress. Research studying the influence of both types of these forces has been limited, and most experiments involving shear stress were comprised of direct instead of transmural shear stress (*43, 44*). Cell-cell interactions can be introduced by multi-layered TEVGs with multiple cell types. In order to investigate the variables

from group 2, a physiological flow system is needed to mimic the natural conditions experienced by SMCs *in vivo*. A multi-layered TEVG with the endothelial and medial layers has been studied under physiological flow conditions, but not in such a way as to decouple the effects of each independent variable (*45*).

Scaffold properties such as mesh size, elastic modulus and degradation rates have all been shown to impact cell activity and the selection of a synthetic scaffold is extremely important in order to study all of the pertinent variables (*46, 47*). PEG hydrogels have both the requisite chemical and physical properties necessary for this research. It is hydrophilic and biocompatible. PEG is permitted for use *in vivo* and has the further benefit of being non-biofouling, meaning it will not adsorb proteins from solution, allowing us to attribute cellular response specifically to the signaling proteins we introduce (*25*). One limitation of PEG hydrogels is that encapsulated cells, even when presented with a scaffold adhesion ligand like RGDS, take on a rounded morphology. Normally, *in vivo*, healthy cell have an elongated phenotype. In hydrogel chemistry, PEG end groups can be modified with acrylate groups yielding PEG diacrylate (PEGDA) for photopolymerized crosslinking. This is advantageous because PEG hydrogels can be formed *in vitro* and implanted, or solution-injected and formed *in vivo*. PEG is chemically modifiable through addition of acrylate molecules, facilitating addition of ECM signaling components such as glycosaminoglycans (GAGs) (*27*). PEG can also be copolymerized with other monomers such as poly(lactic acid) (PLA) and poly(glycolic acid) (PLG) to yield biodegradable gels. Hybrid gels can also be formed

with other polymers such as $PDMS_{star}$ to alter mechanical properties and hydrophilicity (*25*).

To characterize the SMC phenotype, this research will focus on the serum response factor (SRF), a transcription factor and member of the MADS-box family. SRF has been shown to regulate many contractile proteins of SMCs and participates in many cell functions such as proliferation, apoptosis and differentiation. SRF and its binding partners associated with SMCs, myocardin and pelk-1, will give an indication of cell activity and whether it is more directed towards proliferation or differentiation (*48*). Myocardin has been associated with expression of calponin h1, a late term marker for SMC differentiation, while pelk-1 has been shown to have a role in cell growth (*49, 50*). In addition, the efficacy of the different external stimuli will also be assessed by ECM production (collagen and elastin).

1.3.3 Background

Because of the necessity of small diameter vascular tissue replacement and its implications in prolonging life, TEVGs are of growing interest in the biomedical community. TEVGs as a concept were introduced by Weinberg and Bell when they created cell-seeded collagen gel tubes (*51*). This early work was hindered by the need for a synthetic, non-removable support for the tubes. Subsequent attempts also experienced limiting mechanical properties (*52, 53*). The first clinical application was achieved by Shin'oka *et al* using autologous bone marrow cells encapsulated into a

construct created from the biodegradable polymers L-lactide and ε-caprolactone (*54*). These succeeded in low-pressure applications mainly in pediatric patients, but could not be extended to adults and higher pressures. TEVGs for implantation in these systems need mechanical strength similar to that of native tissue and must be able to withstand pressures of >1700mmHg (*36*). They must also be resistant to fatigue since they are exposed to constant cyclic and shear stresses. These factors necessitate the pre-conditioning of SMCs in a synthetic scaffold until they can produce enough natural ECM for stable implantation.

Studies performed with cyclic strain have shown increases in the markers myosin heavy chain (MHC) and h-caldesmon as well as enhanced cell proliferation, all indicative of a more mature phenotype (*55, 56*). ECM production (i.e. elastin and collagen) was also upregulated in the presence of cyclic strain (*57, 58*). Transforming growth factor-β1 (TGF-β1), platelet derived growth factor (PDGF) and vascular derived growth factor (VEGF) were also upregulated in response to cyclic strain (*59, 60*). PDGF and VEGF are an important growth factors involved in angiogenesis. While few studies mimicking the indirect shear stress experienced by SMCs *in vivo* have been performed, some with direct shear have shown significant influence on SMC behavior (*43, 44*). It has been shown that matrix metalloprotease-2 (MMP-2), an enzyme linked to abnormal cell migration, is down regulated while TGF-β1, a major controller of proliferation and differentiation, was upregulated (*43, 44*). Cell-cell interaction studies have also confirmed that in the presence of endothelial cells (ECs) SMCs show increased levels of TGF-β1, PDGF and VEGF (*43*). Basic fibroblast growth factor (bFGF) is thought to be

the key component of embryonic stem cell (eSC) medium acting to maintain the eSCs in an undifferentiated state. Co-culture of SMCs with ECs show decreased levels of this growth factor, suggesting a lowered inhibition to differentiation, leading to a more mature phenotype (*55, 56*).

Past studies on the influence of scaffold mechanical properties have indicated a correlation between modulus and mesh size on cell behavior (*46, 47*). However, these studies were not able to sufficiently decouple the mechanical properties from the biochemical ones. In one instance, scaffold mechanical properties were altered by changing the collagen density in the framework (*61*). Unfortunately, the modulation of collagen density also changes the bioactivity of the scaffold; meaning that comprehensive conclusions as to the actual cause of the changes in cell behavior could not be attributed solely to the change in modulus. In analyzing cell responses to alterations in specific material properties, we will focus on conventional measures of cell ECM deposition and the SRF pathway as a regulator of SMC phenotype. The SRF pathway is an appropriate system to study SMC phenotype and ECM production. Many signaling pathways such as RhoA, TGF-β and MAPK modulate SRF activity, which can control both differentiation and proliferation independently, depending on the presence of particular binding partners (*59, 60*). Myocardin, one such binding partner is a master regulator of SMC gene expression that inhibits differentiation towards skeletal muscle and cell proliferation and will be investigated (*62*). Figure 1.5 is a diagram outlining the path of SMC differentiation from an undifferentiated mesenchyme and shows important early and late-term differentiation markers.

The choice of a cell source is of particular importance when designing TEVGs. The first choice would be vascular smooth muscle cells harvested from the patient. However, due to several factors including persistent disease, hyperplasia and tissue damage, this is not always an option (*63*). Secondly, cells from appropriate animal models could fulfill the demand where autologous cells are unavailable. Common small and large animal models for vascular tissue are rat and pig, respectively. This is also a non-ideal solution given the possibility of an immunoresponse to a foreign cell line. The next logical step would be to harvest a cell type that is undifferentiated, but capable of developing into SMCs upon application of appropriate stimuli. Mesenchymal stem cells (MSCs) fulfill this requisite and can be harvested from various sources within the patient (*64, 65*).

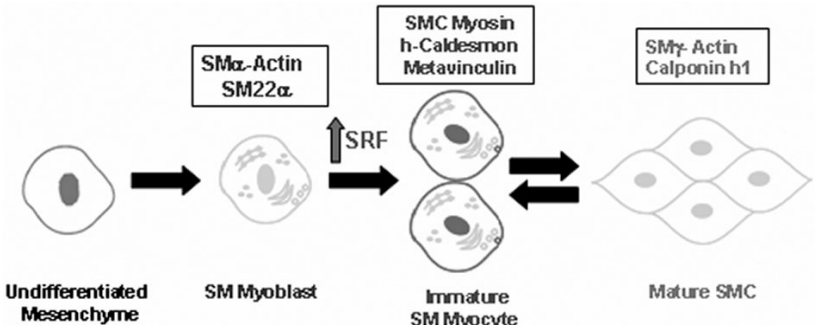

Figure 1.5: SMC differentiation pathway

A common source for MSCs is bone marrow. However, hindrances such as viral infection and decreased cell count with advanced age require other sources to be explored. Advances in harvesting techniques have led to the isolation of MSCs from

many sources such as vascular tissue, umbilical chord blood and processed adipose tissue. MSCs have been shown to differentiate along a myriad of cell lines including osteoblasts, chondrocytes, adipocytes and myocytes (*63-65*). Factors shown to influence SMC behavior and differentiation have also been shown to influence MSC differentiation to SMC (*63, 66-69*). These factors include mechanical stimulation, co-culture with ECs, and exposure to the relevant growth factors and biochemical stimuli. Through the application of previously discussed methods including optimization of artificial scaffold, mechanical conditioning, biochemical interactions and cell-cell interactions, we can selectively differentiate MSCs to SMCs *in vitro* and further optimize their performance as SMCs.

1.3.4 $PDMS_{star}$-PEG Co-Hydrogels

$PDMS_{star}$ materials were developed by the Grunlan group and studied in conjunction with the Hahn group. PDMS can be chemically modified to form crosslinking units similar to those of PEG, allowing for its incorporation into the hydrogel framework. The addition of PDMS significantly expands the range achievable mechanical properties over PEG hydrogels alone. It is hypothesized that this enhanced range of mechanical properties can be achieved without sacrificing the anti-biofouling nature of pure PEG, while introducing control over other scaffold properties including hydrophilicity and elastic modulus. In previous work, amphiphilic materials, such as the one proposed here, have exhibited an ability to limit interaction with biofoulers (*70*). In

general, systematic control over these properties will be achieved by adjusting the weight ratios of the two polymers in solution. $PDMS_{star}$ materials were chosen over a linear molecule because the shape may assist in limiting phase separation between hydrophilic and hydrophobic components (*71*). Figure 1.6 (*72*) shows the co-hydrogels maintaining the non-biofouling property and Figure 1.7 shows a reaction scheme of the formation of $PDMS_{star}$ polymers (*73, 74*).

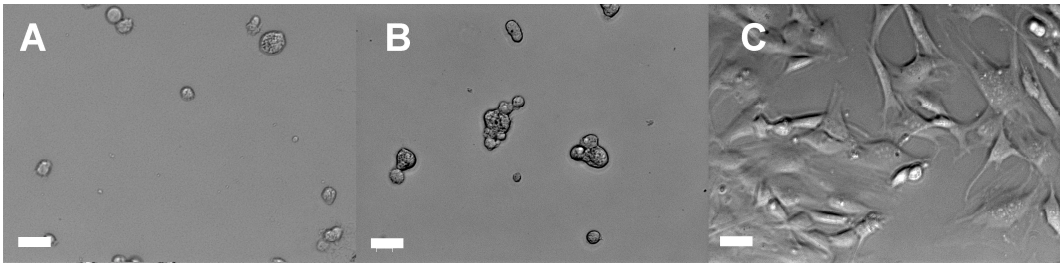

Figure 1.6: Cell spreading on hydrogels: **A:** pure PEG **B:** $PDMS_s$-PEG **C:** $PDMS_{star}$-PEG with 1µmol/mL of RGDS adhesion peptide (*72*)

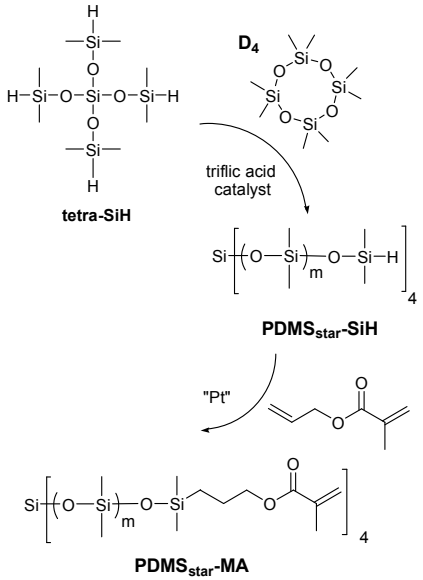

Figure 1.7: Reaction pathway for production of $PDMS_{star}$ diacrylate (*73, 74*)

Previous work with varying ratios of $PDMS_{star}$-PEG, specifically 6 kDa PEG combined in 1:99, 5:95 and 10:90 weight ratios ($PDMS_{star}$:PEG) with 1.8 kDa, 5 kDa and 7 kDa MW $PDMS_{star}$, showed a degree of control over the mechanical properties as well as swelling ratios (indicative of material hydrophilicity). Contrary to what was expected, an increase in MW of $PDMS_{star}$ in the hydrogel resulted in an increase in water uptake. The most likely cause of this is the larger molecular weight resulting in a lower crosslinking density, thereby allowing for greater water absorption.

Preliminary studies also showed differences in extracellular matrix production and expression of differentiation markers. In general, the 5:95 hydrogels showed significant differences from pure PEG in increased collagen and elastin production as well as expression of calponin h1. The other ratios did not show significant differences in extracellular matrix production, but did exhibit differences in the expression of SRF pathway related genes; namely, SRF, calponin h1 and SM γ-actin. The results also suggest a correlation between scaffold modulus and SRF pathway gene expression, consistent with previous studies showing a link between modulus and cell behavior. In an effort to expand on these studies, an expanded property space investigating a wide range of scaffold moduli and swelling ratios is proposed. This expanded property space is represented graphically in Figure 1.8. The mechanical properties span above and below the modulus of native vascular tissue, allowing for the development of optimal *in vitro* culture conditions.

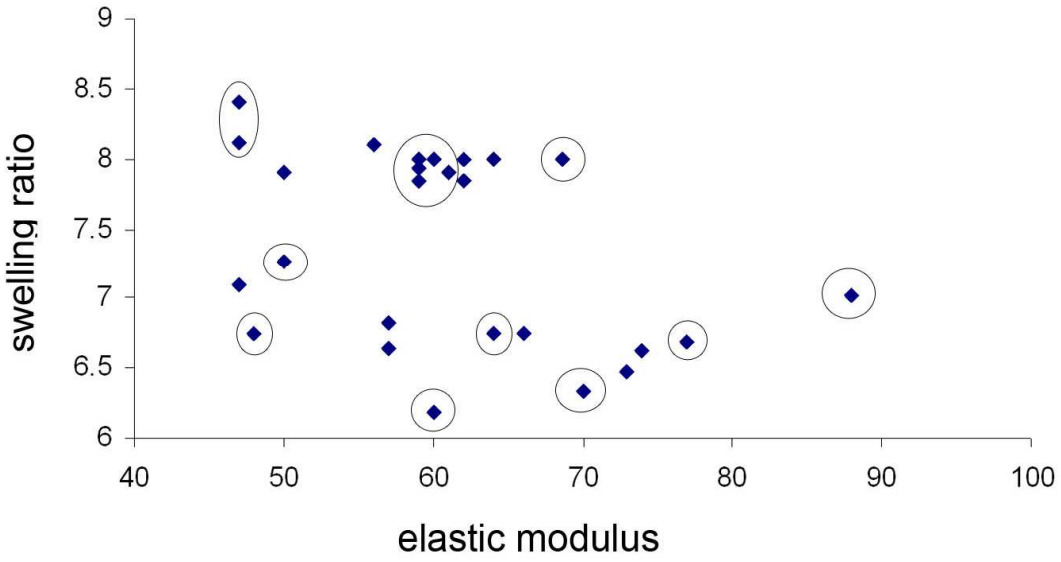

Figure 1.8: 2D property space for $PDMS_{star}$-PEG co-hydrogels with formulations of interest circled

CHAPTER II

MATERIALS AND METHODS

2.1 Introduction

There are many components to consider when analyzing these tissue engineering experiments. Cell behavior can be characterized in many ways including ECM production and deposition along with gene expression. For experiments in which scaffold physical properties are important, these must also be measured. Techniques for analyzing results include histological staining, biochemical assays, reverse transcription-polymerase chain reaction (RT-PCR), Instron tensile testing, and nuclear magnetic resonance (NMR). An example NMR spectrum showing the relevant peaks used to prove acrylation is shown in Figure 2.1. Histological staining will be used to qualitatively and semi-quantitatively assess ECM deposition and gene expression. Biochemical assays will provide a quantitative measure of the same. RT-PCR gives insight into gene expression and related transcription pathways. An Instron 3342 mechanical testing device with a 10N load cell was used to determine the mechanical properties of the hydrogel scaffolds and NMR was employed to calculate the acrylation efficiency as a measure of crosslinking efficiency.

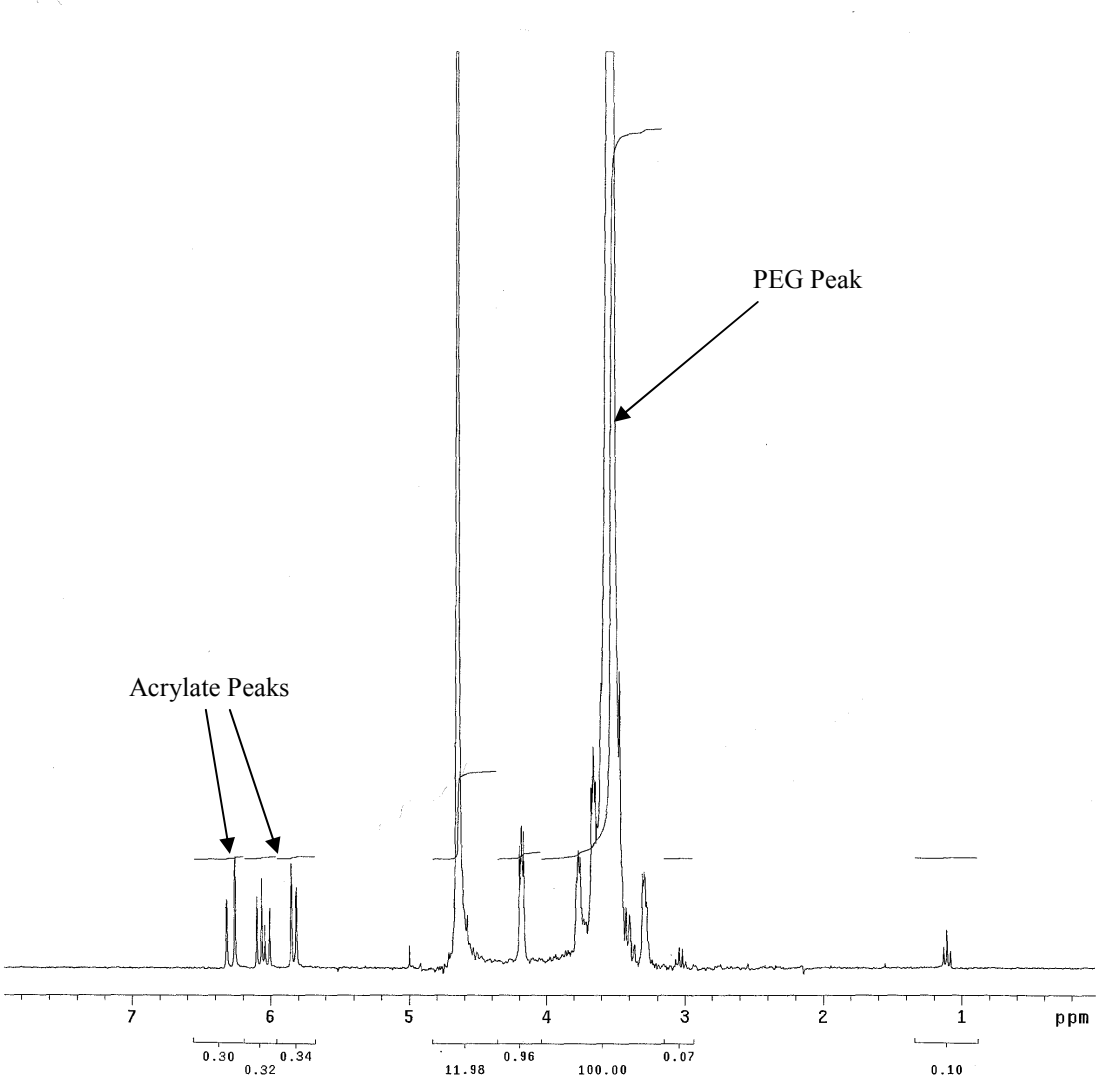

Figure 2.1: Example NMR spectra for PEG acrylation

This research includes: an experiment investigating the impact of biochemical stimuli of GAGs on pig vocal fold fibroblasts (PVFf); three experiments utilizing a physiological bioreactor system to investigate the impact of cell-cell interactions and mechanical conditioning on SMCs in TEVGs; and an experiment employing $PDMS_{star}$-PEG co-hydrogels to measure the impact of scaffold physical properties including elastic

modulus and inorganic content on SMCs for use in TEVGs. General methods for experimental techniques will be presented along with notations for specific experiments where necessary.

2.2 PEGDA Synthesis

PEGDA was prepared as previously described by combining 0.1 mmol/ml dry PEG, 0.4 mmol/ml acryloyl chloride, and 0.2 mmol/ml triethylamine in anhydrous dichloromethane and stirring under argon overnight (*75*). PEGDA of MW 6kDa and 3.4kDa were prepared via this method for use in experiments. The resulting solution was washed with 2 M K_2CO_3 and separated into aqueous and DCM phases to remove HCl. The DCM phase was subsequently dried with anhydrous $MgSO_4$, and PEGDA was precipitated in diethyl ether, filtered, and dried under vacuum.

Cell adhesion peptide RGDS was conjugated to acryloyl-PEG-N-hydroxysuccinimide (ACRL-PEG-NHS) at a 1:1 molar ratio for 2 h in 50 mM sodium bicarbonate buffer, pH 8.5 (*75*). The product (ACRL-PEG-RGDS) was purified by dialysis, lyophilized, and stored at -20 ºC until use.

2.3 $PDMS_{star}MA$ Synthesis

$PDMS_{star}$ methacrylate ($PDMS_{star}MA$) samples were developed and prepared by the Grunlan group. A graphical representation was shown in Figure 1.7 (*73, 74*). All

reactions to synthesize methacrylated star PDMS were run under a N_2 atmosphere with a Teflon-covered stir bar to agitate the reaction mixture. MWs of 1.8, 5 and 7kDa were prepared. Octamethylcyclotetrasiloxane (D_4) was combined with tetrakis(dimethylsiloxy)silane (tetra-SiH) in a 200mL round bottom flask and purged with N_2 for 5mins. They were then reacted by acid catalysis by adding triflic acid to the mixture quickly with stirring for 16h at room temperature (RT). After neutralization with hexamethyldisilazane (HMDS), the polymer was dissolved in minimal toluene and precipitated in methanol (MeOH) at a ratio of 3:1 MeOH:toluene, then dried under vacuum (*73, 74*).

To methacrylate the end groups of the $PDMS_{star}SiH$ polymers, they were first dissolved in 20-35mL of toluene and purged with N_2 in a 250mL round bottom flask. The temperature was raised to 45°C and allyl methacrylate was added dropwise. After raising the solution to 90°C, Karstead's catalyst was added quickly and the mixture was stirred overnight while maintaining the temperature at 90°C (*76, 77*). The final $PDMS_{star}MA$ product needed to be purified and collected. To accomplish this, flash column chromatography was used with a hexanes:ethyl acetate ratio of 2:1 vol:vol, with volatiles removed under reduced pressure. Table 2.1 shows the amounts of reagents used for each desired molecular weight with their subsequent yield of $PDMS_{star}SiH$. Table 2.2 shows the amounts of reagents used to produce $PDMS_{star}MA$ for each molecular weight and their subsequent yields.

Table 2.1: Reagents and yields for synthesis of $PDMS_{star}SiH$

$PDMS_{star}SiH$ $MW_{desired}$ (kDa)	D4 (g/mmol)	tetra-SiH (g/mmol)	triflic acid (µL)	HMDS (g)	$MW_{obtained}$ (kDa)	yield
1.8	30/100	7.8/24	60	0.15	1.8	61%
5	29.9/100	1.7/5	60	0.15	4.6	75%
7	29.9/100	1.1/3.3	60	0.15	6.8	79%

Table 2.2: Reagents and yields for synthesis of $PDMS_{star}MA$

$PDMS_{star}MA$ $MW_{desired}$ (kDa)	allyl methacrylate (g/mmol)	toluene (mL)	Karstedt's catalyst (µL)	yield
1.8	0.42/3.3	35	100	75%
5	1.3/10.2	35	100	94.40%
7	1.6/12.3	35	100	80%

2.4 Cell Culture

The experiments presented here utilized four different cell lines: PVFfs (Cell Applications), rat aortic SMCs (RASMCs Cell Applications), bovine aortic ECs (BAEC, Cell Applications), 3T3 fibroblasts (Cell Applications) and 10T1/2 mesenchymal stem cells (Cell Applications). Each line was thawed and expanded at 37°C and 5% CO_2. The cells were cultured in Dulbecco`s Modified Eagle`s Media (DMEM, Hyclone, Logan) with 10% iron supplemented bovine calf serum (BCS, Hyclone). In addition, PVFfs, RASMCs and BAECs were cultured with 100 mU/mL penicillin, and 100 mg/L streptomycin (Hyclone). A potential concern with using cell lines from different species is a reduction in cell-cell communication, which in TEVGs is an important component in cell behavior. However, this facilitates an easier isolation of cell line effects if cell

migration between layers should occur. RASMCs and BAECs have been used co-currently in many other model systems to study SMC and EC behavior (*78-80*).

2.5 Hydrogel Preparation, Encapsulation and Maintenance

2.5.1 Vocal Fold Experiment

Hydrogel precursor solutions were prepared with 0.1g/mL 10kDa PEGDA and 1μmol/mol ACRYL-PEG-RGDS in HBS (10mM HEPES, 150mM NaCl, pH 7.4) (*75*) and sterilized by filtration. With this procedure, four precursor solutions were prepared, and to one precursor solution each, CSC, HA, HS and DS were added at 1mg/mL. In addition, 10μL/mL of a 300 mg/mL solution of UV photoinitiator 2,2-dimethoxy-2-phenyl-acetophenone (acetophenone, Sigma) dissolved in N-vinylpyrrolidone (Sigma) were added to each solution. PVFfs at passage 8-10 were washed with phosphate buffered saline (PBS), harvested and suspended at $1.6x10^6$ cells/mL in the hydrogel precursor solutions. Precursor solutions were then loaded into a flat plate geometry with a thickness of 1.1mm and photopolymerized under UV light (365 nm, ~10 m mW/cm^2, UVP model B-100SP, Upland) for 2 mins (1min/side). The hydrogel were transferred to Omnitrays (Nunc) fitted with 4 sterile polycarbonate bars to simultaneously prevent gel flotation and prevent gel contact with the tray bottom. Gels were immersed in DMEM supplemented with 10% BCS, 100 μU/mL penicillin, and 100 mg/L streptomycin and

maintained at 37 ºC/5% CO_2 for a period of 17 days. Media was changed every two days until samples were harvested for analysis.

2.5.2 TEVG Experiments

All bioreactor experiments consisted of multi-layered cylindrical constructs. Bioreactors I and II were dual layered experiments utilizing the SMC and EC layers. Bioreactor III was a tri-layered experiment with the additional 3T3 fibroblast layer. The cell lines chosen have been widely used in literature as human vascular models (*81-87*).

2.5.2.1 Bioreactor I

TEVG preparation was similar to that of Bioreactor I, but differs in that instead of a dried monolayer of ECs, the inner layer is a hydrogel cylinder with encapsulated ECs. This required a two step process. First, RASMCs as passages 9-12 were harvested and resuspended at a density of $2x10^6$ cells/mL in the PEGDA hydrogel precursor solution containing 0.1g/mL 6kDa PEGDA and 1μmol/mL ACRYL-PEG-RGDS in HBS-triethanolamine (HBS with 115mM triethanol amine (TEOA)). Ten μl of a 300 mg/mL solution of acetophenone (Sigma) dissolved in N-vinylpyrrolidone (Sigma) was then added per mL of mixture. The resulting solution was sterilized by filtration.

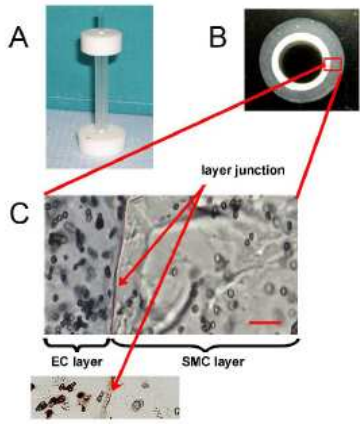

Figure 2.2: Dual-layered vascular graft example. A) Cylindrical mold for TEVG photopolymerization, includes Teflon bases, glass inner rod and plastic outer cylinder. B) Image of a ring segment from a tubular bi-layered PEGDA construct containing SMC in the outer layer and EC in the luminal layer. The luminal layer appears more opaque due to the higher EC seeding density. C) TEVG cross-section showing the outer SMC layer with a higher cell density EC inner layer (*88*)

RASMCs at passages 9-12 were harvested and resuspended at $2x10^6$ cells/mL in the hydrogel precursor solution. The mixture was homogenized and 0.7mL/construct were transferred into the UV transparent cylindrical molds, with an inner diameter of 5mm and an outer diameter of 7.4mm. The solution was photopolymerized under longwave UV light as before for 1min. The inner 5mm rod was removed and replaced by a 4mm glass rod. The constructs were divided randomly. BAECs at passages 9-12 were harvested and resuspended at $10x10^6$ cells/mL in the PEGDA precursor solution. For the first random group, the BAEC-suspended precursor solution was added to the 1mm inner layer at 0.21mL/construct and photopolymerized for an additional 1min. For the second group, the inner layer was composed of a blank PEGDA solution containing no cells at the same volume/construct. For the non-cell containing solution, a volume of

HBS-TEOA equal to that taken up by the cells in the first group was added to the precursor solution to account for volume effects of the cells. Again, the hydrogels in the second group were photopolymerized for an additional 1 min.

The dual-layered hydrogels were removed from their molds and briefly rinsed in PBS containing 1% PSA. Constructs were then immersed in DMEM containing 10% BCS and 1% PSA and were cultured statically at 37 ºC/5% CO_2 for 3 days to ensure contamination did not occur. Media was changed every day until constructs were collected for mechanical conditioning.

2.5.2.2 Bioreactor II

TEVGs created for this experiment follow a similar procedure for those developed in the Bioreactor II experiment. Additionally, there is a third cell layer to introduce and study the effects of 3T3 fibroblasts. This required a three step polymerization process. In addition to the added layer, the cell source will be shifted away from primary smooth muscle cells to the mesenchymal progenitor line, 10T1/2. This line was chosen for multiple reasons. Progenitor cells show greater consistency in behavior over primary cells regardless of source. 10T1/2 cells are well characterized and, like other mesenchymal stem cells, have been shown to differentiate into many cell lines such as osteoblasts, chondrocytes, adipocytes and myocytes, but have shown a preference towards myocytes, or muscle cells (*89-92*). To date, there is still skepticism as to whether or not 10T1/2 cells behave truly as smooth muscle cells upon

differentiation. This work is intended to provide evidence that they can be successfully and selectively guided towards a mature SMC phenotype. The experiment was run with three different configurations with three samples for each; one with all three cell types, one with ECs and 10T1/2 cells, and one with 10T1/2 cells only

3T3 fibroblasts at passage 14-16 were harvested and resuspended at a concentration of $8.6x10^6$ cells/mL in a PEGDA precursor solution (containing 0.1g/mL 6kDa PEGDA and 1μmol/mL ACRYL-PEG-RGDS in HBS-TEOA). Ten μl of a 300 mg/mL solution of acetophenone (Sigma) dissolved in N-vinylpyrrolidone (Sigma) was then added per mL of mixture. The resulting solution was sterilized by filtration. The solution (0.65mL) was then added to a UV transparent mold with an inner glass rod of diameter of 6.9mm and an outer plastic tube with a diameter of 7.4mm and photopolymerized under longwave UV for 1min. For the two sets of constructs without a 3T3 layer, a precursor solution with HBS added in an amount equivalent to the volume occupied by the cells (~0.05mL) was photopolymerized as the outer layer.

10T1/2 mesenchymal stem cells at passage 18-21 were harvested and resuspended at a concentration of $10x10^6$ cells/mL in an equivalent PEGDA precursor solution. The inner glass rod was removed and replaced with one of 4.5mm diameter. The cell-suspended precursor solution (0.55mL/gel) was then added to the cylindrical mold and photopolymerized for an additional 1min. BAECs at passage 9-12 were harvested and resuspended at a density of $7x10^6$ cells/mL. For the two sets that contain an EC layer, the cell-suspended precursor was added to the mold with an inner diameter of 4mm and photopolymerized for an additional 1min. The wall thickness of the inner

layer was reduced to half that of Bioreactor II to closer mimic the EC monolayer present in natural vascular tissue. For the set not containing ECs, the inner layer was photopolymerized with the blank PEGDA precursor solution with an equivalent volume of HBS in place of the BAECs. The tri-layered hydrogels were removed from their molds and briefly rinsed in PBS containing 1% PSA. Constructs were then immersed in DMEM containing 10% BCS and 1% PSA and were cultured statically at 37 ºC/5% CO_2 for 3 days to ensure contamination did not occur. Media was changed every day until constructs were collected for mechanical conditioning.

2.5.2.3 Bioreactor III

Dual-layered TEVGs were prepared with a BAEC inner layer and a RASMC outer layer. In the first step, BAEC cells were locked to the lumen of the construct via drying of the PEGDA precursor solution. Then SMC were encapsulated in the outer area of the tubular PEGDA hydrogels. In conducting this polymerization procedure, a precursor solution containing 0.1 g/mL PEGDA and 1 μmol/mL ACRL-PEG-RGDS in HBS-TEOA (10 mM HEPES, 150 mM NaCl, 115 mM triethanolamine, pH 7.4) was first prepared. Ten μL of acetophenone (Sigma) dissolved in N-vinylpyrrolidone (Sigma) was then added per mL of mixture. The resulting solution was sterilized by filtration.

BAEC at passages 9-12 were harvested and resuspended at $30x10^6$ cells/mL in PEGDA precursor solution. The resulting mixture was spread evenly on a 5mm glass rod (100 μL) and then placed horizontally between two cylindrical molds. Sterile air was

introduced, and the rod was rolled until the viscosity of the PEGDA solution increased substantially to ensure that the cells were anchored. This procedure was repeated to create a uniform monolayer of BAEC cells. The construct was then disassembled and a plastic cylinder (ID = 7.4 mm) was carefully placed over the glass rod. RASMC at passages 9-12 were harvested and resuspended at $2x10^6$ cells/mL in an aliquot of the precursor solution. The resulting mixture was pipetted (~0.7 mL per construct) into the UV transparent cylindrical molds, and polymerization of the PEGDA precursor solution into the tubular hydrogels was initiated by exposure of the molds to UV light (365 nm, ~10 m mW/cm^2, UVP model B-100SP, Upland) for 2 minutes. Figure 2.2 (*88*) shows the cylindrical mold with a dual-layered TEVG.

The resulting hydrogels were removed from their molds and briefly rinsed in PBS containing 1% PSA (10 U/mL penicillin, 10 g/L streptomycin, and 10 g/L amphotericin (Mediatech, Manassas). Constructs were then immersed in DMEM containing 10% BCS and 1% PSA and were cultured statically at 37 ºC/5% CO_2 for 3 days to ensure contamination did not occur. Media was changed every day until constructs were collected for mechanical conditioning.

2.5.2.4 $PDMS_{star}$-PEG Hydrogels

This experiment probes the effects of different scaffold physical properties by introducing $PDMS_{star}$ into the hydrogel network to give wide control over water content, elastic modulus and surface morphology. Twelve different formulations were chosen,

spanning the mechanical properties illustrated in Figure 1.9. Table 2.3 shows the formulations that were chosen and their compositions. For reference, 95:5 refers to a hydrogel with 10% overall polymer concentration in HBS-TEOA, with 95% of that composed of PEGDA and 5% composed of $PDMS_{star}$. In addition, there are two combined formulations of 6kDa and 3.4kDa PEGDA. These also contain an overall polymer concentration of 10% in HBS-TEOA. For example, a precursor solution of each with an overall polymer concentration of 10% in HBS-TEOA, 3.4kDa and 6kDa with 5kDa $PDMS_{star}$ at ratios of 99:1 and 80:20, respectively, were prepared. These were then combined in equal parts to yield the formulation listed in the table. Three samples for each formulation were prepared, yielding 36 total constructs (1 construct of the 6k/5k 90:10 formulation was discarded as a result of contamination leaving 35 total constructs).

10T1/2 mesenchymal stem cells at passage 21 were harvested and resuspended at a density of $3x10^6$ cells/mL in sterile-filtered precursor solutions according to Table 2.3 with an overall polymer concentration of 10% in HBS-TEOA with 1μmol/Ml ACRYL-PEG-RGDS. Precursor solutions (~0.8mL) were added to UV transparent cylindrical molds with Teflon bases. The molds had an outer diameter of 7.4mm with an inner diameter of 5mm. Solutions were then photopolymerized in random groups of three under longwave UV for a period of 5 mins. The tri-layered hydrogels were removed from their molds and briefly rinsed in PBS containing 1% PSA. Constructs were then immersed in DMEM containing 10% BCS and 1% PSA and were cultured statically at

37 ºC/5% CO_2 for a period of 21 days. Media was changed every two days until samples were harvested for analysis.

Table 2.3: Compositions of $PDMS_{star}$-PEGDA hydrogels used to study the effects of scaffold physical properties on SMC behavior. As an example of the ratios presented, 95:5 refers to an overall 10% polymer solution in HBS-TEOA, 95% being PEGDA and 5% being $PDMS_{star}$. For the last two combined formulations, the overall polymer concentration is again 10% in HBS-TEOA, half of which is the 3.4k formulation and half of which is the 6k formulation

PEGDA MW (kDa)	PDMSstarMA MW (kDa)	PEGDA:PDMSstarMA	
3.4	0	100:0	
	1.8	95:5	
	1.8	80:20	
	5	95:5	
	7	99:1	
	7	80:20	
6	0	100:0	
	5	90:10	
	7	80:20	
3.4,6	5	99:1, 80:20	For these formulations, solutions were prepared in equal amounts of the ratios shown, half of the 3.4k formulation and half of the 6k formulation
	5	80:20, 80:20	

2.6 Mechanical Conditioning

The three bioreactor experiments include a period of mechanical conditioning to study its effects on SMC behavior and 10T1/2 differentiation in addition to those effects introduced by cell-cell interactions. Figure 2.3 (*41*) shows a schematic of the physiological flow system used for these experiments. The system, described previously (*41*), consists of a bioreactor chamber which houses the TEVGs, which are surrounded by culture media (DMEN, 10% BCS, 1% PSA). A Masterflex L/S digital peristaltic

pump with two Easy Load II pump heads (Cole Palmer) generates flow by drawing media from the reservoir. The media then flows through a compliance chamber followed by a pulsatile pump (CellMax, Spectrum Labs) which was used to overlay the sinusoidal waveform (Figure 2.4) (*88*). Media then flowed through the inner lumen of the TEVG constructs to mimic the constant mechanical conditioning experienced by vascular tissue *in vivo*.

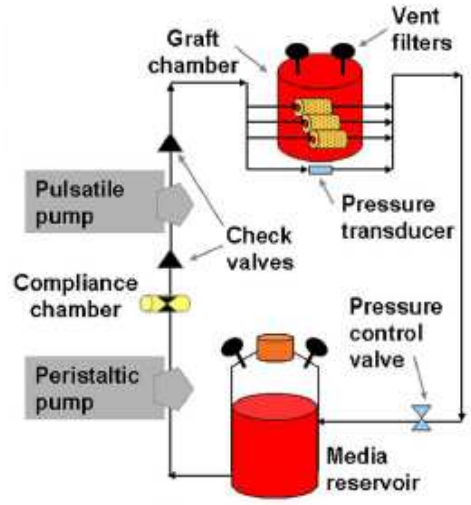

Figure 2.3: Physiological flow system to control mechanical conditioning in TEVGs. The system consists of a bioreactor chamber to house constructs, peristaltic pump to provide flow, and a pulsatile pump to provide the sinusoidal waveform. Reactor chamber and media reservoir are vented to the atmosphere to maintain pressure and allow for gas exchange (*41*)

The media reservoir and reactor chamber were outfitted with sterile gas-exchange filters to maintain an atmospheric pressure and maintain constant CO_2 levels.

Constructs maintained sealed contact with the bioreactor fittings via their internal elasticity. Previous work (*39*) has indicated that fetal pulsatile conditioning enhance blood vessel formation; therefore, conditions resembling those of human late gestation with mean pressures of ~50mmHg, amplitudes of ~20mmHg and 140-180 beats per minute (bpm) were chosen (*93, 94*).

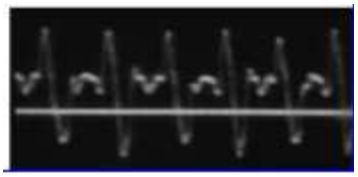

Figure 2.4: Representative sinusoidal waveform for bioreactor experiments. Amplitutde and frequency mimic those of late human gestation (*88*)

To measure system pressures, in-line pressure transducers (one per chamber) were introduced. Media flow then returned to the reservoir. This system setup allows for systematic, concurrent control over all parameters including flow rate, pulse frequency, overall pressure and pressure amplitude. All system components, except for presterilized pressure transducers, were autoclaved and assembled in a sterile, laminar flow hood.

2.6.1 Bioreactor I

This experiment consisted of two bioreactors, with six constructs containing both the SMC and EC layer and six constructs containing only an SMC layer. In each bioreactor, three constructs were mechanically conditioned and three were kept under static conditions. Constructs from this experiment will further be denoted as EC+/dyn+ for dynamic constructs with an EC layer, EC-/dyn+ for dynamic constructs without an EC layer, EC+/dyn- for static constructs with an EC layer, and EC-/dyn- for static constructs without an EC layer. For the first three days of experimentation, the flow rate was increased to 360 Ml/min (120 Ml/min per construct) in 40 Ml/min increments, while mean pressures increased to ~50mmHg. On day 4, pulsation was introduced yielding an average waveform of 60/40mmHg at a frequency of ~160bpm to achieve the late human gestation conditions. Media was changed every 2-3 days to replenish nutrients, stabilize Ph and prevent contamination. The bioreactors were run for a total period of 21 days, after which samples were harvested for analysis.

2.6.2 Bioreactor II

Three construct types were utilized in this experiment. The first set contained all three cell types (EC, SMC, fibroblast), the second set contained the EC and SMC layers, and the third set contained only the SMC layer. All constructs were run under dynamic conditions and the following nomenclature will be used to refer to the different

constructs for discussion: Fib+/EC+, Fib-/EC+, Fib-/EC-. Reactor 1 contained Fib-/EC- constructs, reactor 2 contained Fib+/EC+ constructs and reactor 3 contained Fib-/EC+ constructs. The experiment was run for a total period of 18 days. Over the first five days, the overall flow rate was slowly increased to 360 Ml/min (120 Ml/min per construct) in ~40Ml/min increments. Pulsation was introduced on day 4. After achieving full flow, the average waveforms were 128/100, 120/90 and 120/90 mmHg for reactors 1, 2 and 3, respectively, with a pulsation frequency of ~160bpm. Media was changed every 2-3 days to replenish nutrients, stabilize Ph and prevent contamination. After the experiment's completion, samples were harvested for analysis.

2.6.3 Bioreactor III

This experiment was performed with three constructs run under dynamic mechanical conditioning and three constructs left under static conditions. Media was changed every 2-3 days to replenish nutrients, stabilize pH and prevent contamination. The system was run for a total period of 15 days. For the first 7 days, flow was slowly and systematically ramped from 60 Ml/min to a final flow rate of 360 Ml/min, yielding an average flow of 120 Ml/min per construct. Pulsation was introduced at day 4, and the average waveform was 65/40mmHg with ~160bpm when full flow was achieved on day 9. After 15 days, samples were collected from both dynamic and static constructs, which will be denoted as dyn+ and dyn- for results discussion.

2.7 Sample Collection

2.7.1 Vocal Fold Experiment

After the duration of the experimental run, samples were collected by taking circular rings with a sterile 8mm punch. Samples were briefly washed in PBS with 1% PSA. Half of the samples were then placed in sterile 1.5Ml tubes, frozen by liquid N_2 and stored at -80°C until analysis. The other half were taken for mechanical testing and subsequently stored at -80°C for further analysis.

2.7.2 Bioreactor Experiments

After completion of each experimental run, samples were collected in the following manner. Each construct was cut into ~6 cylindrical segments at ~4-6mm in length. The ends of each construct were discarded. For bioreactors II and III, the inner luminal layer was removed to avoid interference of the ECs in sample analysis. Samples allocated for Qrt-PCR and western blot assays were immediately transferred to RNA-later (Ambion) to preserve RNA. These samples were then stored at 4°C overnight and subsequently transferred to -80°C. The remaining segments for each construct were washed with PBS for immediate mechanical testing and later histological analysis.

2.7.3 $PDMS_{star}$-PEG Hydrogels

Following the experimental run, gels were transferred to PBS and cut into 6 segments. End sections were used for mechanical analysis. One section from each was transferred to a 1.5Ml tube, frozen immediately in liquid N_2 and stored at -80°C. One section from each was cut and transferred immediately to RNA-later, stored at 4°C overnight and transferred to -80°C. Samples taken for histological analysis were transferred to Tissue Tek culture media (Sakura Finetek), stored at 4°C overnight and transferred to -20°C until use. Mechanical testing samples were then taken for immediate analysis on an Instron 3342 mechanical testing device.

2.8 Mechanical Testing

All samples were analyzed on an Instron 3342 mechanical testing device equipped with a 10N load cell.

2.8.1 Vocal Fold Experiment

Samples with dimensions of 8mm diameter and 0.55mm thickness were tested under compression to determine elastic modulus.

2.8.2 TEVG Experiments

Samples for TEVG experiments were tested under tension to determine elastic modulus. The technique used was an application of the circumferential property testing developed and validated for accuracy in previous works (*95, 96*). This technique approximates the area of force application on the ring segments as two rectanges, with sides equal to the width and wall thickness of the ring (measured by calipers). The gauge length, l_{gauge}, was calculated as the diameter of the ring at half wall thickness. Strain was then determined by the equation $\Delta l/l_{gauge}$ (eq1) and the modulus was calculated by the stress-strain output from the testing device after applying a uniaxial strain rate of 6mm/min. Figures 2.5 and 2.6 show example output graphs of Bioreactor III, with the stress range of interest taken to be 10-25 kPa. The measured elastic moduli could then be used to estimate the transmural strain experienced by the grafts under mechanical conditioning in the bioreactor. The following equation adapted from the Bernoulli equation: $\varepsilon = \frac{\Delta P\, r_v}{h_v E}$ (eq2), where ε = strain, ΔP = peak-to-trough pressure rise, E = elastic modulus, r_v = vessel inner radius, and h_v = vessel wall thickness (*97*). This method has been successfully applied to estimate circumferential strains experienced by PEG hydrogel in previous works (*41*). Wall shear stress was estimated by the Hagen-Poiseuille equation (*98*): $\Delta P = \frac{8\mu L Q}{\pi r^4}$ (eq3), where ΔP = pressure drop, L = length of pipe, μ = dynamic viscosity, Q = volumetric flow rate, and r = radius.

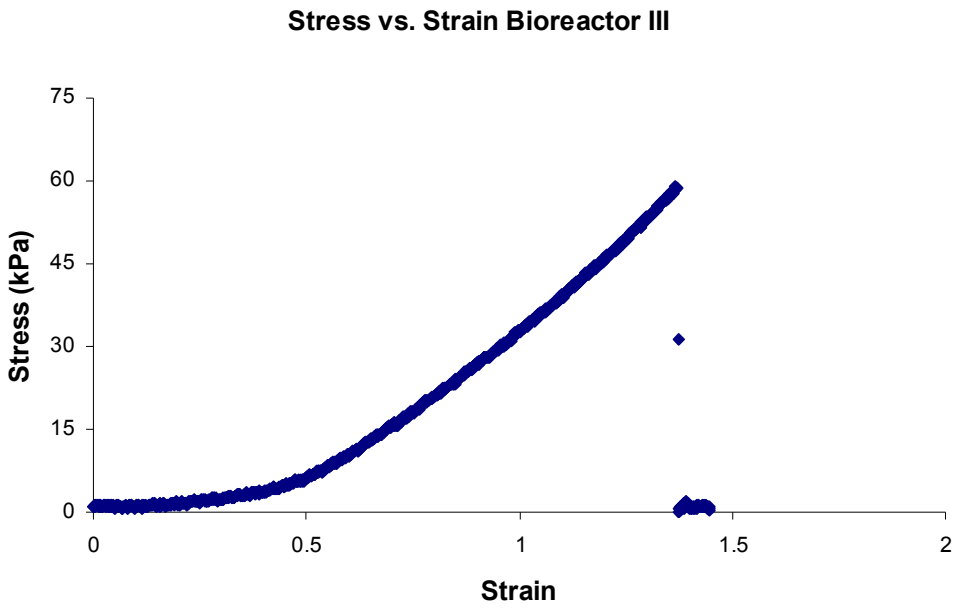

Figure 2.5: Stress/strain curve for approximation of TEVG elastic modulus

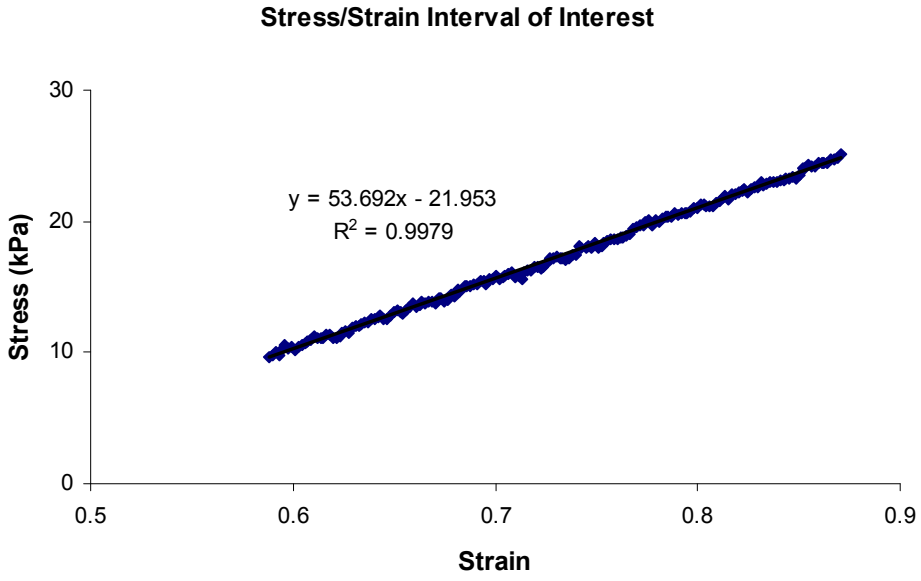

Figure 2.6: Stress/strain interval from 10-25kPa for estimation of TEVG elastic modulus

2.9 Biochemical Analysis

Samples used for biochemical analysis had previously been snap frozen in liquid N_2 and stored at -80°C until use. For every test performed, standards were also encapsulated in equivalent PEGDA hydrogels and digested before analysis to account for any differences that hydrogel encapsulation may introduce.

2.9.1 DNA Analysis

DNA analyses were performed as an assessment of the number of cells present upon experimental completion. This gives an assessment of overall cell viability inside the hydrogels. Samples from the hydrogels were thawed, weighed, digested in 10N NaOH and neutralized. The DNA content of each sample was then determined using the PicoGreen assay (Invitrogen). A conversion factor of 6.6pg DNA/cell was used to convert resultant DNA content to total cell number with calf thymus DNA (Sigma) used as a standard (*41*).

2.9.2 Sulfated GAG Anlaysis (sGAG)

The Blyscan assay (Biocolor) was used to measure the total sGAG production. 80Ml of each sample (digested by 10N NaOH) were neutralized and combined with

120Ml Blyscan dye reagent. Immediately following addition of the dye, the absorbance at 525nm was measured and quantified in relation to CSC-B (Sigma) as a standard.

2.9.3 Collagen Analysis

Collagen production was estimated by hydroxyproline levels within the hydrogel samples. Samples were hydrolyzed for 18h at 110°C in 6N HCl and subsequently dried by centrivap (Labconco). After completion of the drying step, samples were resuspended in DI H_2O and was reacted with chloramine T and p-dimethylbenzaldehyde as previously described (*99*). L-4-hydroxyproline was used as a standard, and samples were read at 550nm and quantified relative to the standard. The total collagen content was then obtained by dividing total hydroxyproline by 0.13.

2.9.4 Elastin Analysis

As described in previous work, elastin levels were determined by a ninhydrin assay (*100*). Following digestion at 100°C in 10N NaOH, samples were pelleted and further digested in 6N HCl at 110°C for 18h and subsequently dried by centrivap. The remaining amino acids were boiled in the ninhydrin reagent, cooled and read at 570nm (*41*), and quantified using α-elastin (MP Biochemicals) as a standard. In addition to the ninhydrin assay, direct ELISA can also be used to analyze cellular elastin production. Sample digestion was accomplished with 0.1M NaOH for 24h at 37°C. Samples were

then neutralized and further digested with 0.25M oxalic acid at 100°C overnight. Microcon YM-3 centrifugal filters (Millipore) were used to exchange oxalic acid for PBS. Following exchange, 100μL of each sample were added to a high binding EIA 96 well plate (Nunc) for 3h at RT. The primary elastin antibody (clone B4) was applied followed by donkey anti-mouse HRP secondary antibody and 2,2'-azino-bis(3-ethylbenzthiazoline-6-sulphonic acid) (Sigma). Samples were analyzed at 410nm and quantified relative to bovine aortic elastin (Sigma) as a standard.

2.10 Histological Analysis

All samples assigned for histological analysis were frozen in Tissue-Tek media (Sakura Finetek) before cutting on a Jung CM 1800 cryogenic cutting device (Histotronix) at 35μm thickness. Samples were first fixed with 10% formalin for 10min followed by Peroxidaze (Biocare Medical) treatment for 10min. Sections were then blocked with Terminator (Biocare Medical) for 10 min and then exposed to the primary antibody for 1h. The secondary antibody was then applied for 30min followed by application of a detection kit. Table 2.4 shows the primary antibodies with their respective concentrations in HBS. Table 2.5 shows the different secondary antibodies used and their corresponding detection kits.

Table 2.4: List of antibodies used in histological staining, RT-PCR and Western blotting with antibody type, source and staining dilution

Antibody	Type	Source	Satining Dilution
Collagen I	Rabbit IgG	Rockland	1:20
Collagen II	Rabbit IgG	Rockland	1:20
Collagen III	Rabbit IgG	Rockland	1:20
Elastin (BA-4)	Mouse IgG	Santa Cruz	1:20
Myo-d (c20)	Rabbit IgG	Santa Cruz	1:20
GAPDH (V18)	Goat IgG	Santa Cruz	N/A
SM α-actin (1A4)	Mouse IgG	Santa Cruz	1:20
SM γ-actin (B4)	Mouse IgG	Santa Cruz	1:20
Osteocalcein (fl-95)	Rabbit IgG	Santa Cruz	1:20
SRF (G-20)	Rabbit IgG	Santa Cruz	1:20
Myocardin (h300)	Rabbit IgG	Santa Cruz	1:20
Elk-1 (i-20)	Rabbit IgG	Santa Cruz	1:20
Calponin (N-15)	Goat IgG	Santa Cruz	1:20
Fibrillin (c-19)	Goat IgG	Santa Cruz	1:20
c-Fos (4)	Rabbit IgG	Santa Cruz	1:20
c-Jun (h79)	Rabbit IgG	Santa Cruz	1:20
p-elk-1 (B4)	Mouse IgG	Santa Cruz	1:20
CD-34 (C-18)	Goat IgG	Santa Cruz	1:20
Sk/cd α-actin (5c5)	Mouse IgG	Santa Cruz	1:4
PCNA (pc10)	Mouse IgG	Zymed	1:20
PKC (A-3)	Mouse IgG	Santa Cruz	1:20
pERK	Mouse IgG	Santa Cruz	1:20

Table 2.5: Secondary antibodies used in histological staining, RT-PCR and Western blotting with secondary anti-body type, source, staining dilution, detection kit and positive detection stain

Secondary Antibody	Source	Staining Dilution	Detection Kit	Stain
Universal Link IgG	Biocare	N/A	4+ HRP	Chromogen AEC
Donkey anti-mouse IgG HRP	Santa Cruz	1:20	4+ HRP	Chromogen AEC
Donkey anti-mouse IgG AP	Santa Cruz	1:20	N/A	Chromogen Ferangi Blue
Donkey anti-rabbit IgG-AP	Santa Cruz	1:20	N/A	Chromogen Ferangi Blue
Donkey anti-rabbit IgG-HRP	Santa Cruz	1:20	4+ HRP	Chromogen AEC
Goat anti-mouse IgM-HRP	Santa Cruz	1:20	4+ HRP	Chromogen AEC
Donkey anti mouse AP	Jackson	1:50	N/A	Chromogen Ferangi Blue
Donkey anti rabbit AP	Jackson	1:50	N/A	Chromogen Ferangi Blue
Donkey anti mouse HRP	Jackson	1:50	4+ HRP	Chromogen AEC
Donkey anti rabbit HRP	Jackson	1:50	4+ HRP	Chromogen AEC
Donkey anti goat HRP	Jackson	1:50	4+ HRP	Chromogen AEC

Histological stainings for elk1, myocardin and AFABP required exposure to a buffer solution (100Mm NaCl, 300Mm sucrose, 3Mm $MgCl_2$, 10Mm HEPES, 0.5% Triton-100X) prior to application of the primary antibody. Stained sections were then observed both qualitatively and quantitatively through an Axiovert microscope (Zeiss). To quantify the results, the total number of cells was compared to the total number of positively stained cells for each individual staining.

2.11 RNA Isolation

Samples were stored at -80°C in RNA-later until use. They were transferred to 2Ml screw-cap microfuge tubes containing 1.5Ml of Trizol reagent and 1Ml of 3.2mm diameter stainless steel beads. Homogenization was accomplished through cycling the tubes at 4800rpms in 10s cycles followed cooling on ice. The tubes were then centrifuged and the supernatants collected and mixed with chloroform (Sigma), shaken for 15s and centrifuged again.

The aqueous phase from each tube was separated from the phenol-chloroform phase, which was extracted and stored at -20°C for later protein isolation. Isopropanol, with Rnase-free glycogen as a carrier, was used to precipitate the RNA. The RNA pellet was washed with 75% and then 95% ethanol and subsequently exposed to Dnase (Qiagen) at 37°C for 30min. The mixture was then held at 70°C for 5min to inactivate the Dnase, then cooled on ice. RNA was again precipitated by 10Ml of 3M sodium acetate (Ph 5.5)

followed by 275Ml of 100% ethanol per 100Ml of mixture. The pellet was again washed each with 75% then 95% ethanol and resuspended in 51Ml of Rnase-free water.

2.12 qRT-PCR

Superarray provided the proprietary Qrt-PCR primers for rat myocardin, calponin h1 and GAPDH, and efficiencies of ~1 were verified. Each sample was measured with a Biorad i-Cycler detection system (Biorad) and the SuperScript III Platinum One-Step Qrt-PCR kit (Invitrogen). 6 Ml of template and 5Ml of primer were added per 25Ml of reaction mixture. SYBR Green fluorescence was used as a basis for monitoring the amplification during the PCR phase with a threshold value for exponential phase of amplification determined using MyiQ software (Biorad). The threshold was marked and used to determine the C_t or amplification cycle for each sample. For the constructs the following equation was used to quantify gene expression levels relative to the housekeeping gene GAPDH: $2^{-\Delta Ct,gene}=2^{-(Ct,gene-Ct,GAPDH)}$. The average $2^{-\Delta Ct,gene}$ for the EC-/dyn+ constructs was used to normalize the other groups' $2^{-\Delta Ct,gene}$ averages. Results were verified by melting curve analysis and agarose gel elctrophoresis.

2.13 Western Blotting

2.13.1 Protein Isolation

Protein isolation was conducted by the method set forth in previous work (*101*). The phenol-chloroform phase from the RNA extraction procedure was mixed with ethanol to precipitate the remaining DNA. The liquid phases were dialyzed in 3.4kDa SnakeSkin dialysis membranes (Pierce) for 60h at 4°C against aqueous 0.1% sodium dodecyl sulfate (SDS) while changing the buffer solution every 18-20h. A tri-phase mixture resulted, yielding a globular mass as the phase of interest. This phase was collected and resuspended in PBS with 0.5% SDS and 1% Triton X-100.

2.13.2 Blotting Procedure

A 10% SDS-PAGE gel was used to separate 10μg of total protein per sample at 180V for 1h, which were then transferred to nitrocellulose membranes (Pierce) at 25V for 1.5h. The membrane was blocked with TBS-BSA (Tris-buffered saline and 3 wt% bovine serum albumin) and primary antibodies were diluted in the same buffer and applied overnight at 4°C with constant rotation. The primary antibodies were detected with donkey anti-mouse-IgG-HRP or donkey anti-rabbit-IgG-HRP (Jackson Immunoresearch) with subsequent application of luminal chemiluminescent reagent

(SCBT). The signal was detected using Kodak X-Omat LS Film (Kodak) (*88*). Table 2.5 shows the proteins detected and the corresponding primary antibodies used.

2.13.3 Semi-quantitative Procedure

To quantitatively assess the results of the blotting, intensities of developed films were detected with a high-resolution optical scanner (Dell). Each protein band was analyzed for optical density using the GelPlot2 Macro of Scion Image software (Scion). For elastin, the primary antibody chosen recognizes mature elastin as well as three iso-forms of tropoelastin, yielding separate bands for the different proteins. The tropoelastin bands were ignored and only the mature elastin was analyzed for comparison between constructs. GAPDH was used as a normalizing basis, and each protein band density was divided by its corresponding GAPDH band.

2.14 Statistical Analysis

Data are reported with a mean and corresponding standard deviation. Comparisons between samples were accomplished through the use of ANOVA and Tukey's *post hoc* test (SPSS). A $p < 0.05$ was taken as the basis for statistical significance.

CHAPTER III

VOCAL FOLD EXPERIMENT

3.1 Introduction

ECM components have received increasing recognition of their importance in cell behavior and function. They have been shown to influence several areas including osmosis, cell migration, differentiation, molecular transport and molecular concentration (*102, 103*). The ECM consists of traditional structural support components such as collagen and elastin, as well as interstitial components composed primarily of glycans and proteoglycans, or GAGs. HA has been widely studied and is considered one of the most important GAGs in terms of influencing cells of the vocal fold, especially in functions such as wound healing (*102, 103*). Other GAGs that may also prove to be influential over vocal fold cell behavior, such as CSC, DS and HS, have not been as widely studied. This work seeks to increase understanding of the effects of different proteoglycans on vocal fold cells, specifically PVFfs. PVFfs were chosen as bovine cells have been used widely as a human model in tissue engineering (*99, 104*).

Vocal fold fibroblasts interact with ECM proteoglycans through surface receptors. The most common surface receptor identified in vocal fold tissue is CD44, and it has been identified as a primary surface protein in fibroblasts, hematopoietic cells and tumor cells (*105-108*). CD44 has been widely studied in its relation as a surface receptor for HA, but has also received recognition as a significant surface receptor for

DS, HS and CSC as well (*108-112*). In addition, CD44 in VFfs is responsible for controlling the extracellular signal-related kinase (ERK) and protein kinase C (PKC) transcription pathways, important for the regulation of VFfs. The work presented here seeks to expand understanding of GAG influence over VFf behavior and function. PVFf were encapsulated in 10kDa PEGDA and studied for potential effects of GAG presence over the ERK and PKC transcription pathways and their control over ECM deposition.

3.2 Experimental

A brief experimental will be presented here. For a more detailed description, see the relevant methods sections in Chapter II. Hydrogel precursor solutions were prepared with 0.1g/mL 10kDa PEGDA and 1μmol/mol ACRYL-PEG-RGDS in HBS (10mM HEPES, 150mM NaCl, pH 7.4) and sterilized by filtration (*75*). With this procedure, four precursor solutions were prepared, and to one precursor solution each, CSC, HA, HS and DS were added at 1mg/mL. In addition, 10μL/mL of a 300 mg/mL solution of acetophenone (Sigma) dissolved in N-vinylpyrrolidone (Sigma) were added to each solution. PVFfs at passage 8-10 were washed with phosphate buffered saline (PBS), harvested and suspended at $1.6x10^6$ cells/mL in the hydrogel precursor solutions. Precursor solutions were then loaded into a flat plate geometry with a thickness of 1.1mm and photopolymerized under UV light (365 nm, ~10 m mW/cm^2, UVP model B-100SP, Upland) for 2 mins (1min/side). The hydrogel were transferred to Omnitrays (Nunc) fitted with 4 sterile polycarbonate bars to simultaneously prevent gel flotation

and prevent gel contact with the tray bottom. Gels were immersed in DMEM supplemented with 10% BCS, 100 μU/mL penicillin, and 100 mg/L streptomycin and maintained at 37 ºC/5% CO_2 for a period of 17 days. Media was changed every two days until samples were harvested for analysis.

After the duration of the experimental run, samples were collected by taking circular rings with a sterile 8mm punch. Samples were briefly washed in PBS with 1% PSA. Half of the samples were then placed in sterile 1.5Ml tubes, frozen by liquid N_2 and stored at -80°C until analysis. The other half were taken for mechanical testing and subsequently stored at -80°C for further analysis. Samples were analyzed for mechanical properties immediately following sample collection. ECM analysis included collagen I, III and elastin. Collagen types I and III are the primary collagen components of the vocal folds. Total collagen was determined via the hydroxyproline assay, while individual collagen types were determined by histological staining with quantitative cell counting. Elastin production was analyzed through direct ELISA. Histological stainings were also performed and quantified for SMα-actin, an indication of vocal fold scarring, proliferating cell nuclear antigen (PCNA), a cell-proliferation marker, pERK and PKC.

3.3 Results and Discussion

Figure 3.1 shows the results of scaffold mechanical testing. From the figure, it is clear that the mechanical properties of the DS gels differ significantly from the other formulations. Scaffold physical properties have significant influence over cell behavior.

Since the goal of this experiment was to study GAG influence, and for the DS formulation, the mechanical properties cannot be decoupled from other influential components, results from this formulation will be ignored in the experimental analysis.

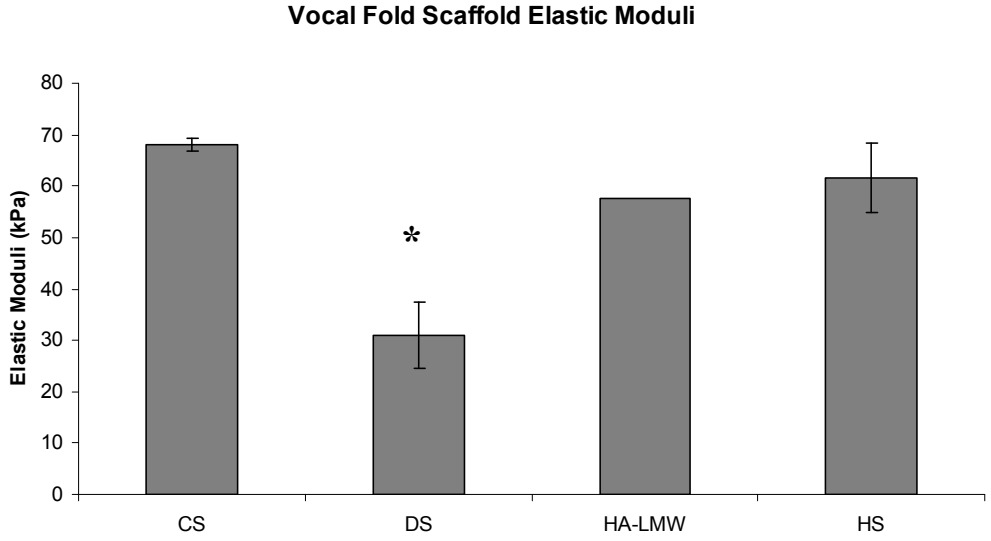

Figure 3.1: Mechanical properties for individual PEGDA formulations modified with selected GAGs. The DS formulation shows significant deviation from the other three formulations, and thus will not be included in the experimental analysis

Figures 3.2 and 3.3 show the total collagen production (biochemical analysis), collagen I and collagen III (histological staining), respectively. While total collagen production is consistent, it can be seen from Figure 3.3 that the individual collagen types differ significantly between formulations. Collagen I production was enriched in CSC and HS gels (HS enrichment not statistically significant), while collagen III was enriched in HA gels. In natural vocal fold tissue, the ratio between collagen I and III production is approximately 1, indicating some effect of the HS and CSC proteoglycans on the fibroblast signaling process.

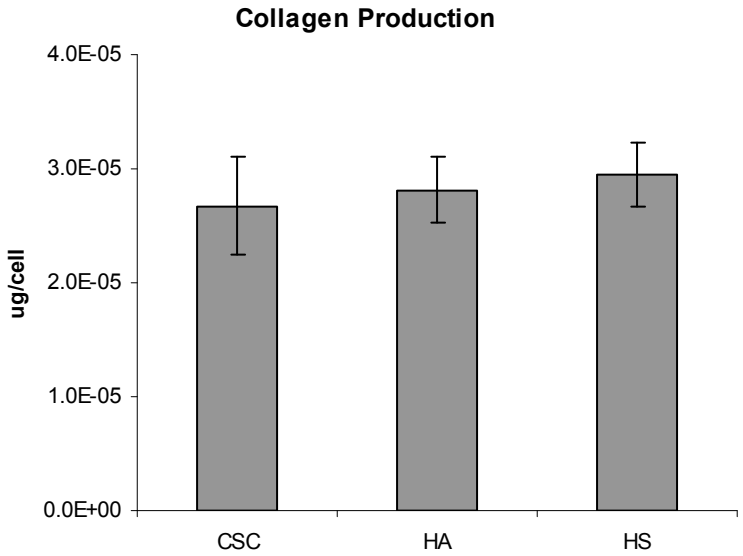

Figure 3.2: Total collagen production by hydroxyproline assay. No significant different exists between selected formulations

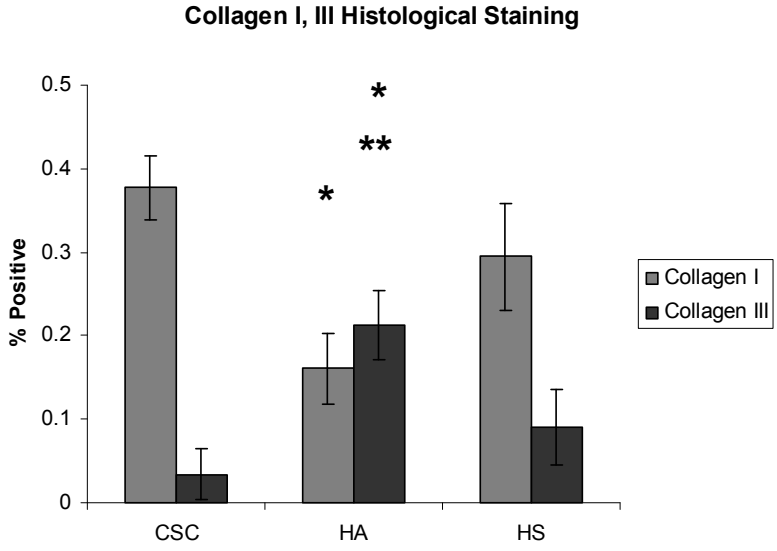

Figure 3.3: Collagen I and III production quantified by histological staining and cell counting. *Significant difference between HA and CSC formulations. **Significant difference between HA and HS formulations

Figure 3.4 contains elastin production data obtained from direct ELISA. No significant differences exist between the formulations, indicating the proteoglycans do not affect VFf elastin production.

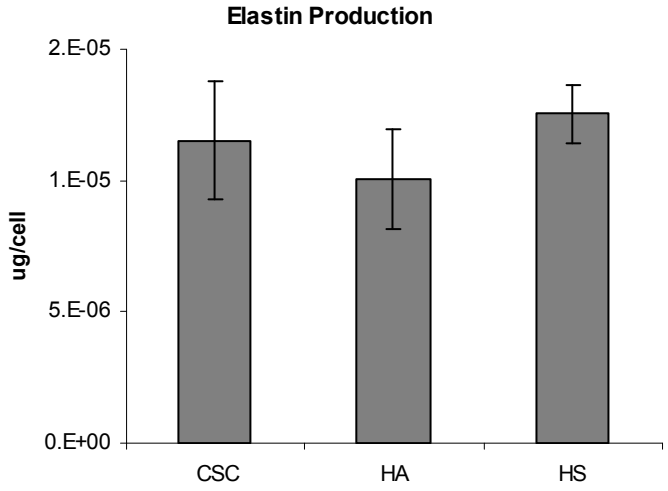

Figure 3.4: Elastin production as measured by direct ELISA

Figures 3.5 and 3.6 show results for ERK and PKC, respectively. ERK shows significant differences for both CSC and HA from HS, while PKC histological stainings showed no significant differences. This could indicate influence ERK signaling over collagen production, but results are not detailed enough to draw comprehensive conclusions.

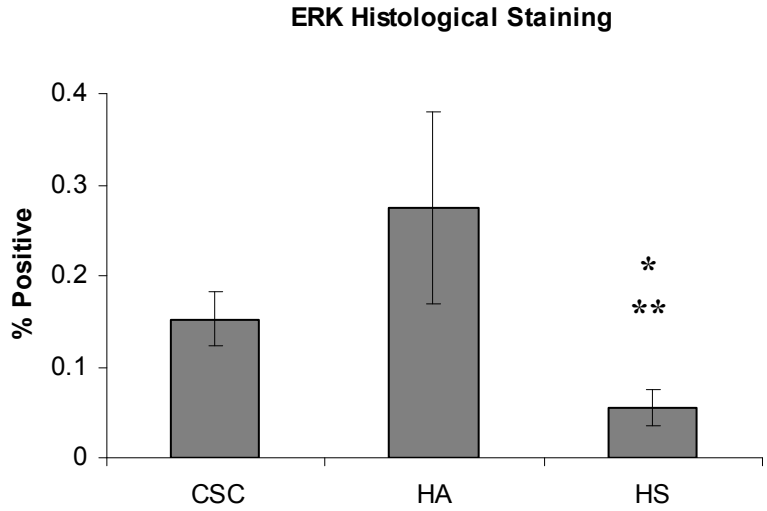

Figure 3.5: ERK expression quantified by histological staining and cell counting. *Significant difference between HS and CSC formulations. **Significant difference between HS and HA formulations

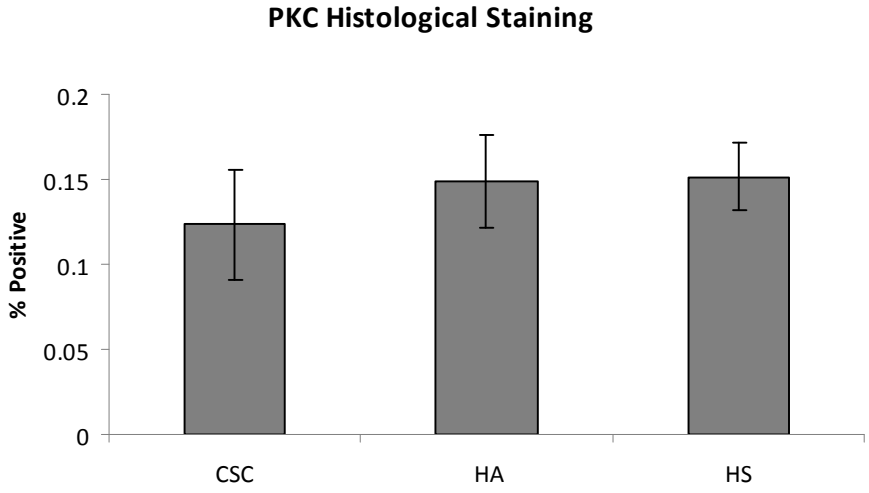

Figure 3.6: PKC expression quantified by histological staining and cell counting

SM α-actin and PCNA expression results are shown in Figures 3.7 and 3.8, respectively and were obtained via histological staining and cell counting. Results for PCNA show no significant difference, but staining for SM α-actin show enhanced levels

in both the HS and CSC formulations. This trend follows the levels of ERK expression, indicating a potential correlation. High levels of SM α-actin are associated with vocal fold scarring and generally present during wound healing. Increased expression of wound healing markers would be expected in replacing damaged tissue, but enhanced levels of SM α-actin would be generally undesirable.

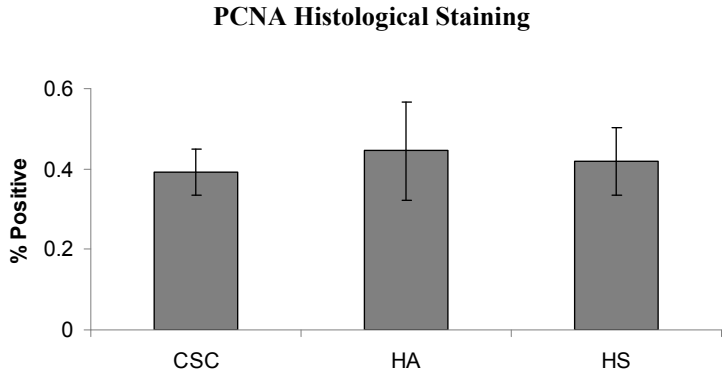

Figure 3.7: PCNA expression quantified by histological staining and cell counting

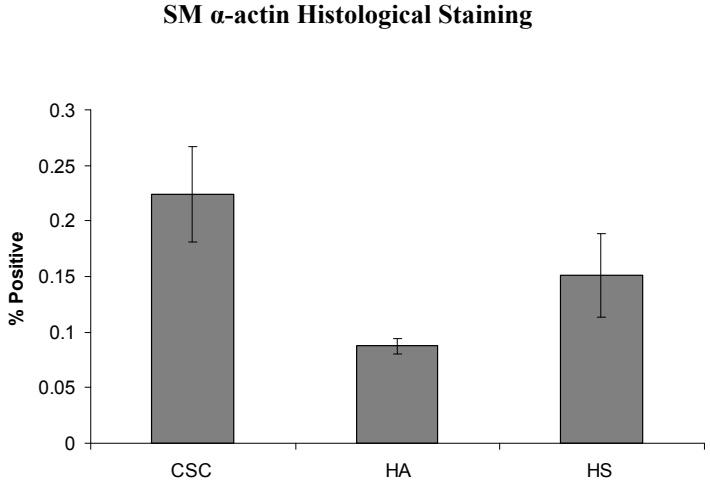

Figure 3.8: SM α-actin expression quantified by histological staining and cell counting

CHAPTER IV

MECHANICAL CONDITIONING AND EC PRESENCE ON RASMC

4.1 Introduction

TEVGs have received strong attention in recent years as a potential replacement for damaged, small diameter (<6mm) vascular tissue (*6, 38-41, 88*). Cell-cell interactions as well as mechanical conditioning, including both cyclic strain and shear stress, have been shown to have a significant impact on SMC behavior. Under physiological conditions, vascular tissue undergoes constant mechanical stimulation, experiencing both cyclic strain and shear stress. The shear stress experienced by SMCs *in vivo*, however, is an indirect, transmural stress, rather than a direct stress (*6, 40, 41*). They are surrounded by ECM, and are further buffered from direct contact with the conditioning fluid by an EC layer. Few studies mimicking this type of stress and strain conditioning have been conducted, and the research presented here seeks to create a comprehensive physiological flow system that mimics *in vivo* conditions and can be systematically tuned to give control over pressure waveforms and flow rate. The system setup was shown in Figure 2.2 and is reproduced here. The individual, decoupled effects of mechanical conditioning and EC presence were studied. Instead of a dry EC monolayer, ECs were encapsulated in a thin hydrogel as a separate layer in the constructs. This deviates from natural vascular tissue where ECs are present in a monolayer, but facilitates easy removal of the luminal layer for a focused analysis of the

SMC layer. EC+ and EC- constructs were run under both dynamic and static conditions and analyzed for SMC phenotype and ECM production.

PEG hydrogels were chosen because of their biocompatibility, ease of modification and biological "blank slate" nature (*25, 113*). The experimental setup presented here allows for independent study of the impact of both EC presence as well as mechanical conditioning. This was accomplished through the creation of dual-layered hydrogels that mimic the multi-layered structure of natural vascular tissue, with an EC monolayer surrounded by an SMC medial layer. Hydrogels were synthesized through photopolymerization of PEG with modified acrylate end groups.

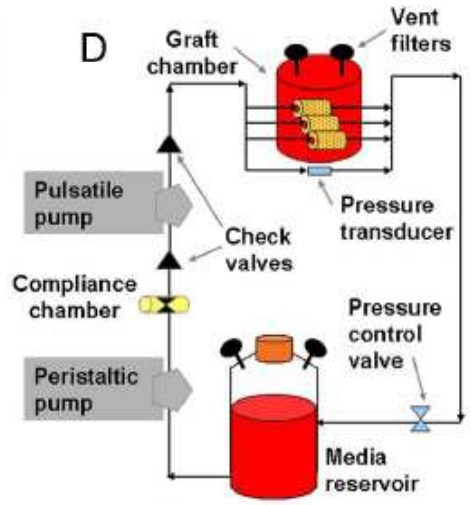

Figure 2.2: Physiological flow system to control mechanical conditioning in TEVGs. The system consists of a bioreactor chamber to house constructs, peristaltic pump to provide flow, and a pulsatile pump to provide the sinusoidal waveform. Reactor chamber and media reservoir are vented to the atmosphere to maintain pressure and allow for gas exchange (*41*)

4.2 Experimental

A brief experimental will be presented here. For a more detailed description, see the relevant methods sections in Chapter II (Bioreactor I). A PEGDA precursor solution (0.1g/mL 6k PEGDA, 1μmol/mL ACRYL-PEG-RGDS, and 10μL/mL acetophenone in HBS-TEOA) was prepared and sterilized by filtration. RASMCs as passage 9-12 were harvested and resuspended at $2x10^6$ cells/mL in the precursor solution and photopolymerized in a UV transparent cylindrical mold with an outer diameter of 7.4mm and an inner diameter of 5mm (~0.7 mL/construct) for 1 min. The inner rod was removed and replaced with a 4mm glass rod. For half of the constructs, BAECs at passage 9-12 were harvested and resuspended in the precursor solution at $10x10^6$ cells/mL and added to the cylindrical mold, creating a wall thickness of 1mm. The remaining grafts were completed with an inner layer composed of the precursor solution without cells. The inner layer was photopolymerized for an additional 1min.

The dual-layered hydrogels were removed from their molds and briefly rinsed in PBS containing 1% PSA. Constructs were then immersed in DMEM containing 10% BCS and 1% PSA and were cultured statically at 37 ºC/5% CO_2 for 3 days to ensure contamination did not occur. Media was changed every day until constructs were collected for mechanical conditioning.

This experiment consisted of two bioreactors and twelve constructs. In one bioreactor, constructs were EC+, with half being run as dyn+ and half being run as dyn-. In the remaining bioreactor, constructs were EC-, with half run as dyn+ and half run as

dyn-. For the first three days of experimentation, the flow rate was increased to 360 Ml/min (120 Ml/min per construct) in 40 Ml/min increments, while mean pressures increased to ~50mmHg. On day 4, pulsation was introduced yielding an average waveform of 60/40mmHg at a frequency of ~160bpm to achieve the late human gestation conditions. Media was changed every 2-3 days to replenish nutrients, stabilize Ph and prevent contamination. The bioreactors were run for a total period of 21 days, after which samples were harvested for analysis.

Constructs were cut into ring segments. End segments were discarded. Samples for biochemical analysis were snap frozen in liquid N_2 and stored at -80°C until use. Samples for RNA analysis were diced, transferred to RNA-later, stored at -20°C overnight and moved to -80°C until analysis. Samples designated for histological analysis were frozen in Tissue Tek media at -20°C. Samples for mechanical conditioning were rinsed with PBS and immediately tested for elastic modulus. Analyses were performed probing both SMC phenotype and ECM production. Histological staining was performed for ECM proteins collagen I, III and elastin. Staining for differentiation markers myocardin, calponin h1 and elk-1 were also performed along with SRF expression. As an additional measure of differentiation marker expression, qRT-PCR was performed for myocardin and calponin h1. A semi-quantitative procedure using Western blots was also performed to give further insight into collagen I, III, elastin, SRF and elk-1 presence.

4.3 Results and Discussion

Mechanical testing data yielded similar results for all groups of constructs. Figure 4.1 shows the average elastic modulus with standard deviation for each formulation. No statistically significant differences were observed. Applying eq2, average circumferential strains of 6% were obtained, with an average pressure amplitude of 20 mmHg. Applying eq3, wall shear stresses were calculated to be ~1 dyn/cm^2 in dynamic constructs. The mechanical data obtained allow the effects of mechanical conditioning and cell-cell interactions to be decoupled from scaffold physical properties.

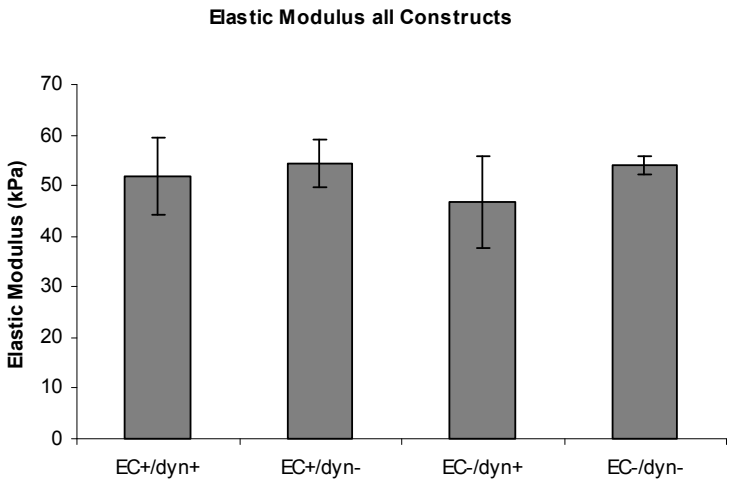

Figure 4.1: Mechanical data for all construct formulations. No statistically significant differences were observed

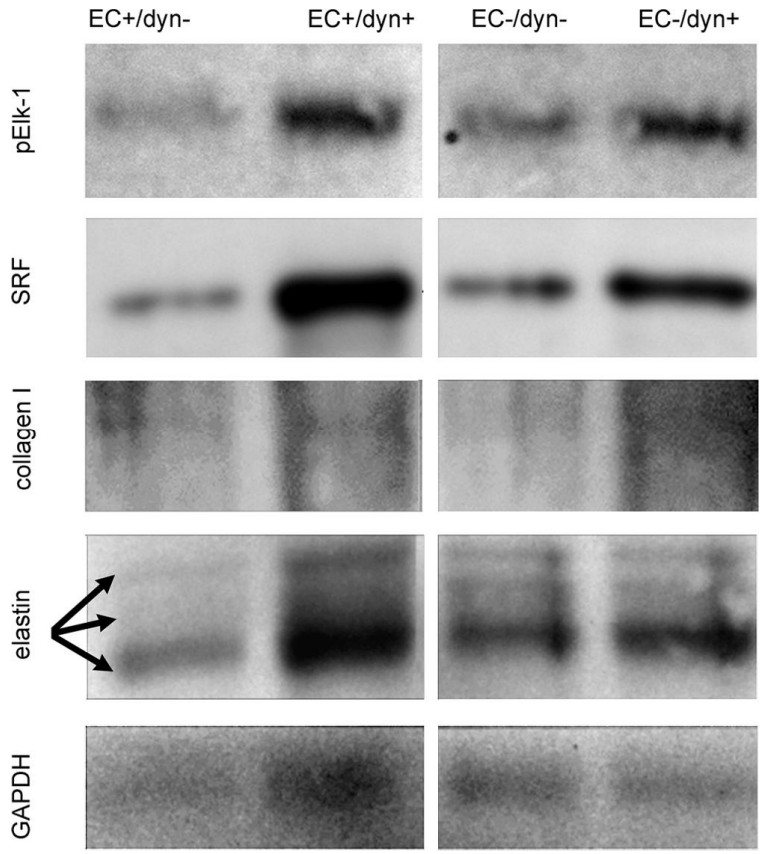

Figure 4.2: Representative immunoblots for differentiation markers and ECM deposition (*88*)

ECM deposition analysis was performed by semi-quantitative Western blotting (Figure 4.2) and cell counting of histological staining. Production of collagen I, III and elastin was measured and is presented in Figure 4.3 (*88*). Western blots were completed and developed over film, which was then optically analyzed for quantitative comparison. After optical analysis, average values for each protein were divided by the optical density value for GAPDH, chosen as a housekeeping gene. For comparison between immunoblots, films were internally normalized to the average EC-/dyn+ ratio.

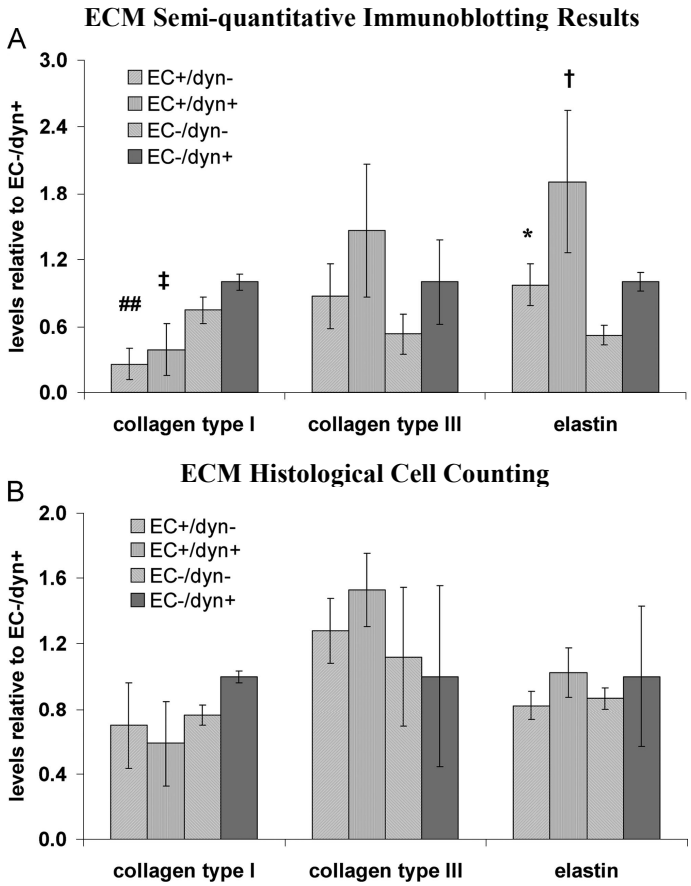

Figure 4.3: Quantitative results for ECM deposition. A) Western blotting results. B) Histological staining. *Statistically significant difference between EC+/dyn- and EC+/dyn+. †Significant difference between EC+/dyn+ and EC-/dyn-. ‡ Significant difference between EC+/dyn+ and EC-/dyn+. ##Significant difference between EC+/dyn- and EC-/dyn+ (*88*)

From Figure 4.3A, elastin production increased in EC+/dyn+ constructs relative to EC-/dyn- and EC+/dyn- constructs, indicating that mechanical conditioning influences elastin deposition. For collagen I, EC+ constructs showed diminished production. From Figure 4.3B, the trends from the quantitative histology generally agree with those from the immunoblotting. However, standard deviations are too large to draw statistical

conclusions. Combined ECM results indicate different modulation from EC presence and mechanical conditioning independently. Combining EC presence with dynamic conditioning reduced collagen I production while enhancing elastin production. Previous work has also indicated a reduction in total collagen production with EC+ TEVGs undergoing pulsatile conditioning (*45*). However, the previous work did not isolate diminished collagen production specifically to collagen I. Ratios between collagen I and III in vascular tissue has significant impact on tissue mechanical properties, with enriched collagen III tissues identified as more elastic (*114*). Further work must be done to investigate the underlying signaling pathways controlling collagen production to attempt to block any collagen I reduction. While the decoupled effects of mechanical conditioning in EC- constructs did not show significant increase in ECM production, this is likely do to a limited sample number, and reducing standard deviations may bring results into line with previous work (*40, 57, 60, 115, 116*).

Figure 4.4 (*88*) shows quantitative results for SRF, elk-1, myocardin and calponin. SRF and elk-1 were analyzed via Western blots and histological staining. Myocardin and calponin h1 were analyzed via qRT-PCR and histological staining. EC presence and mechanical presence independently enhanced SRF expression. Specifically, EC+/dyn+ constructs showed greater SRF expression relative all other formulations.

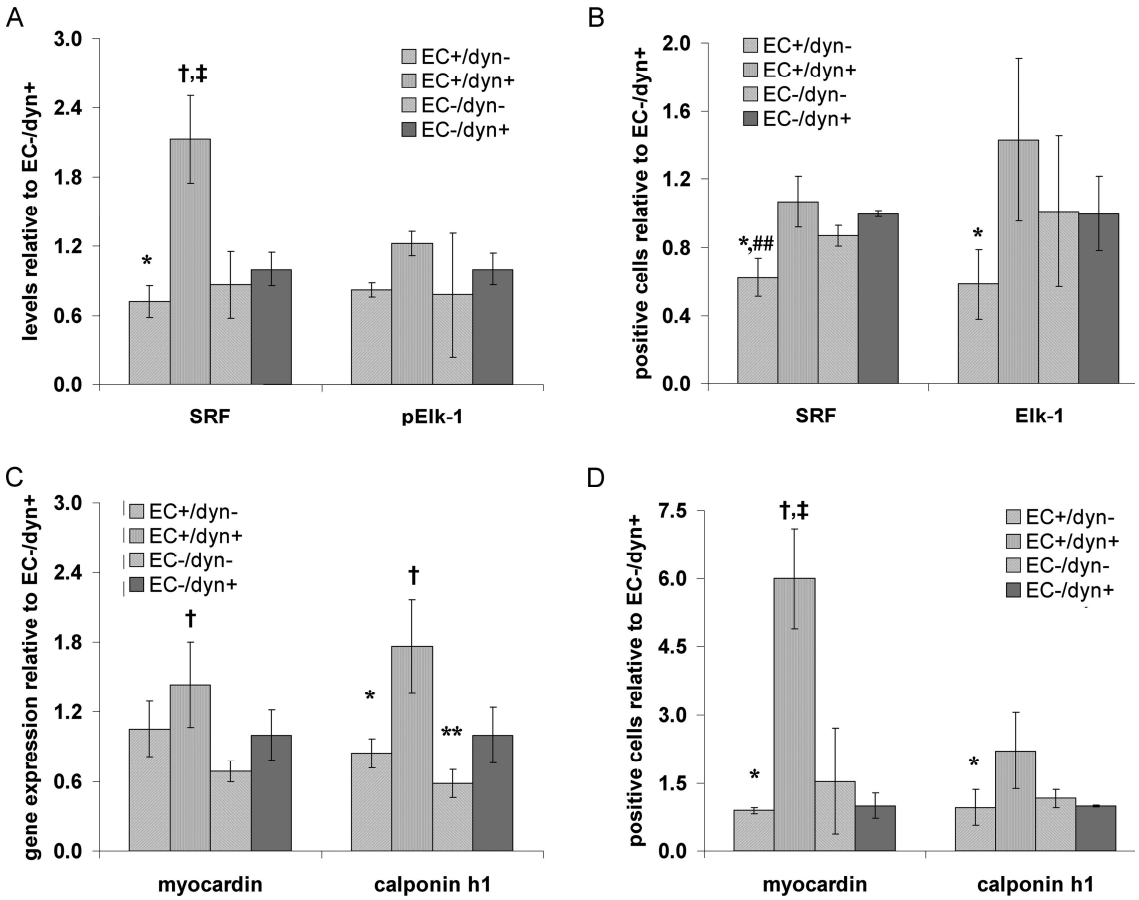

Figure 4.4: Quantitative results for SRF, elk-1, myocardin and calponin h1. A) SRF and elk-1 quantified by Western blot. B) SRF and elk-1 quantified by histological staining. C) Myocardin and calponin h1 quantified by qRT-PCR. D) Myocardin and calponin h1quantified by histological staining. *Significant difference between EC+/dyn- and EC+/dyn+ constructs. **Significant difference between EC-/dyn- and EC-/dyn+ constructs. †Significant difference between EC+/dyn+ and EC-/dyn- constructs. ‡Significant difference between EC+/dyn+ and EC-/dyn+ constructs. ##Significant difference between EC+/dyn- and EC-/dyn+ constructs (*88*)

Analysis for elk-1 by immunoblot showed no statistically significant differences. SRF analysis by histology showed enhanced expression in EC+/dyn+ over EC+/dyn- constructs, indicating an influence of mechanical conditioning over expression of this transcription factor. Elk-1 analysis by histology showed similar enhancement in EC+/dyn+ constructs. Overall, these results agree with the trends observed through

Western blots. Figure 4.5 (*88*) shows representative histological staining for each construct type for collagen I, III, elastin and calponin h1.

qRT-PCR for calponin h1 showed enhanced expression in dyn+ constructs over dyn- constructs. Calponin h1 was also enhanced most effectively in EC+/dyn+ constructs. Myocardin expression was enhanced in EC+/dyn+ constructs relative to the EC-/dyn- constructs. Histological staining results agreed in general with those obtained through gene expression. Calponin expression was enhanced in EC+/dyn+ relative to EC+/dyn- constructs, while EC+/dyn+ constructs were significantly enhanced over all other formulations. These combined results indicate that both EC presence and mechanical conditioning enhance SMC differentiation. Myocardin promotes calponin h1 expression, which preferentially drives SMC differentiation, while elk-1 competes with myocardin as an SRF binding partner and promotes proliferation (*48-50, 62*). Therefore, it can be expected that an increase in the myocardin:elk-1 ratio would enhance calponin h1 expression. These results are in agreement with previous work (*56, 117*).

Immunostaining was also performed for traditional EC markers, vWF and NOS. The results showed localized production of each to the luminal layer, indicating minimal to no cell migration between layers. Representative images of these stainings can be seen in Figure 4.6 (*88*). The localization of the EC layer is important, because it allows for conclusions for SMCs in the medial layer to be drawn without interference from EC-produced proteins.

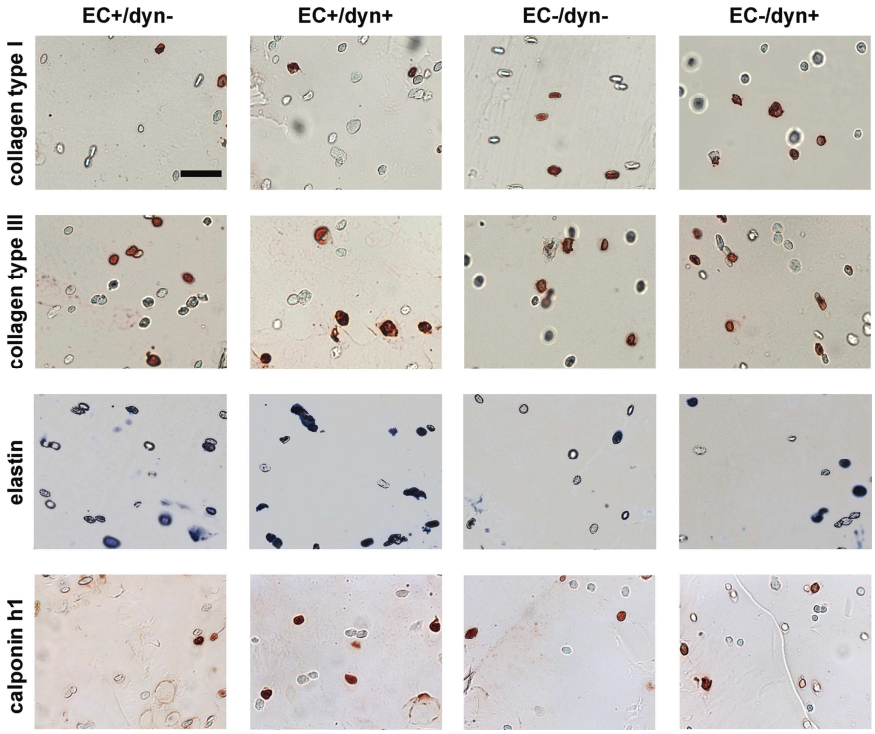

Figure 4.5: Representative histological staining for collagen I, III, elastin and calponin h1. For collagen I, III and calponin h1, positive staining is red, while for elastin, positive staining is blue (*88*)

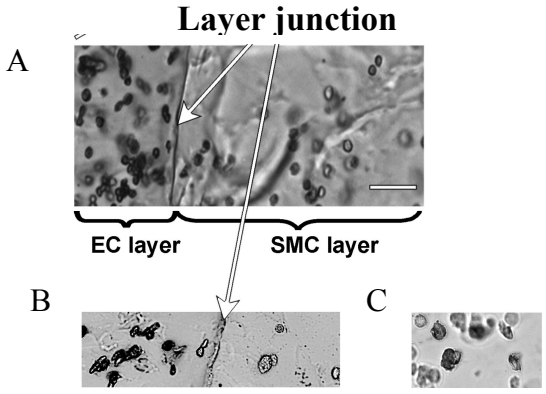

Figure 4.6: Representative images of EC/SMC boundary layer. A) Unstained section of dual-layered TEVG. B) Dual-layered construct stained for vWF showing localized position of ECs. C) EC section stained for NOS to show EC functionality. Positive stainings are black (*88*)

CHAPTER V

MECHANICAL CONDITIONING, EC AND FIBROBLAST PRESENCE ON MSCs

5.1 Introduction

This experiment expands on the results obtained in previous bioreactor experiments by introducing the adventitial, or fibroblast layer of vascular tissue into the TEVGs. Additionally, RASMCs will be replaced by 10T1/2 mesenchymal stem cells. Mesenchymal stem cells are undifferentiated progenitor cells capable of maturing into several different lines including myocytes, chondrocytes, adipocytes, osteoblasts and SMCs (*63-65*). They are an attractive option for TEVGs because they are available from multiple sources throughout the potential patient's own body, eliminating the need for the introduction of a foreign cell line into the body, thus minimizing risk of rejection and inflammatory response. Similar factors affecting SMC phenotype and ECM production, including mechanical conditioning and inter-cell communication, have also been shown to influence mesenchymal stem cells (*66-68*). Progenitor cells have also shown greater consistency in behavior over primary cells regardless of their source, and are well characterized (*89-92*). This experiment will attempt to decouple the effects of the adventitial layer on SMC behavior from mechanical conditioning. One additional change was the thickness of the EC layer, which has been reduced from 1mm to 0.5mm to more closely resemble the monolayer of natural vascular tissue.

5.2 Experimental

A brief experimental will be presented here. For a more detailed description, see the relevant methods sections in Chapter II (Bioreactor II). A PEGDA precursor solution (0.1g/mL 6k PEGDA, 1μmol/mL ACRYL-PEG-RGDS, and 10μL/mL acetophenone in HBS-TEOA) was prepared and sterilized by filtration. 3T3 fibroblasts at passage 14-16 were harvested and resuspended at $8.6x10^6$ cells/mL in the precursor solution. The solution (0.65mL/construct) was then added to a UV transparent cylindrical mold with an inner glass rod of diameter 6.9mm and an outer plastic tube of diameter 7.4mm for 1/3 of constructs. The solution was photopolymerized under longwave UV for 1min. The inner rod was removed and replaced by a rod of diameter 4.5mm.

10T1/2 mesenchymal stem cells at passage 18-21 were harvested and resuspended at a concentration of $10x10^6$ cells/mL in the precursor solution. The solution (0.55mL/gel) was then added to the cylindrical mold and photopolymerized for an additional 1min. The inner rod was removed and replaced by a rod of 4mm. BAECs as passage 9-12 were harvested and resuspended at $7x10^6$ cells/mL in the precursor solution. The solution was then added to the mold and photopolymerized for an additional 1min. For another 1/3 of constructs, the fibroblast layer was replaced by blank PEGDA precursor solution and was prepared with a 10T1/2 layer and a BAEC layer. For the final 1/3 of constructs, the fibroblast and BAEC layers were replaced with blank PEGDA precursor solution, leaving only the medial 10T1/2 layer. The tri-layered

hydrogels were removed from their molds and briefly rinsed in PBS containing 1% PSA. Constructs were then immersed in DMEM containing 10% BCS and 1% PSA and were cultured statically at 37 ºC/5% CO_2 for 3 days to ensure contamination did not occur. Media was changed every day until constructs were collected for mechanical conditioning.

A three reactor system was used in this experiment to accommodate the three construct types. Reactor 1 contained fib-/EC- constructs, reactor 2 contained fib+/EC+ constructs and reactor 3 contained fib-/EC+ constructs. The experiment was run for a total period of 18 days. Over the first five days, the overall flow rate was slowly increased to 360 Ml/min (120 Ml/min per construct) in ~40Ml/min increments. Pulsation was introduced on day 4. After achieving full flow, the average waveforms were 128/100, 120/90 and 120/90 mmHg for reactors 1, 2 and 3, respectively, with a pulsation frequency of ~160bpm. Media was changed every 2-3 days to replenish nutrients, stabilize Ph and prevent contamination. After the experiment's completion, samples were harvested for analysis. Constructs were cut into ring segments. End segments were discarded. Samples designated for histological analysis were frozen in Tissue Tek media at -20°C. Samples for mechanical conditioning were rinsed with PBS and immediately tested for elastic modulus.

5.3 Results and Discussion

Mechanical testing results are shown in Figure 5.1. No significant difference exists between constructs. This allows for the elastic modulus to be removed as an

experimental variable. Figures 5.2 and 5.3 show quantitative histological staining results for collagen and elastin deposition, respectively. Standard deviations are too high to make statistical conclusions, but some general trends can be observed.

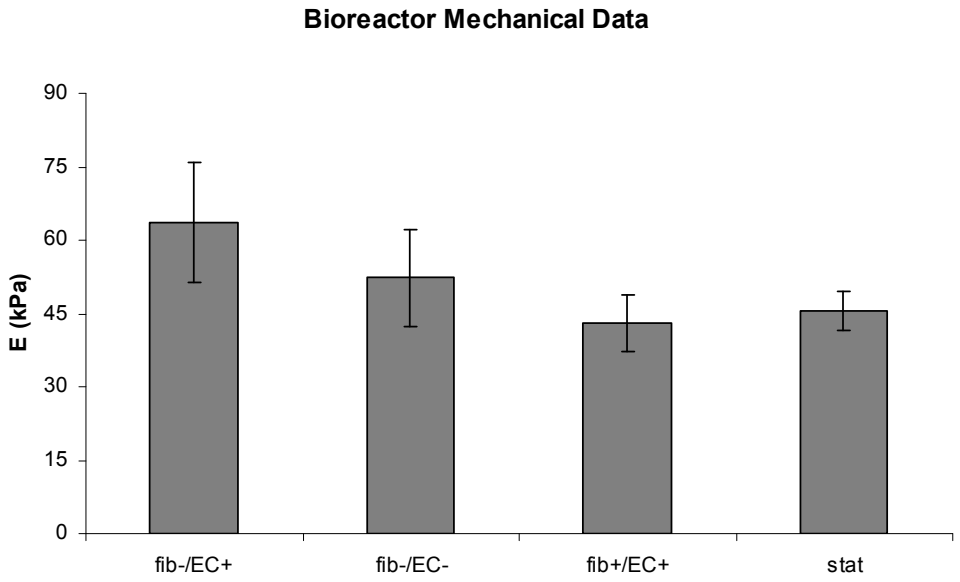

Figure 5.1: Construct elastic moduli. No statistically significant differences were observed

Deposition of collagen I and III were similar on average. This is in contrast to the previous experiment which showed a decrease in collagen I production with EC presence. Collagen II is indicative of a chondrocyte phenotype. Collagen II was overall diminished by presence of EC and fibroblasts, and further reduced by dynamic conditioning. This indicates that physiological conditions inhibit 10T1/2 cells from differentiating towards a chondrocyte phenotype.

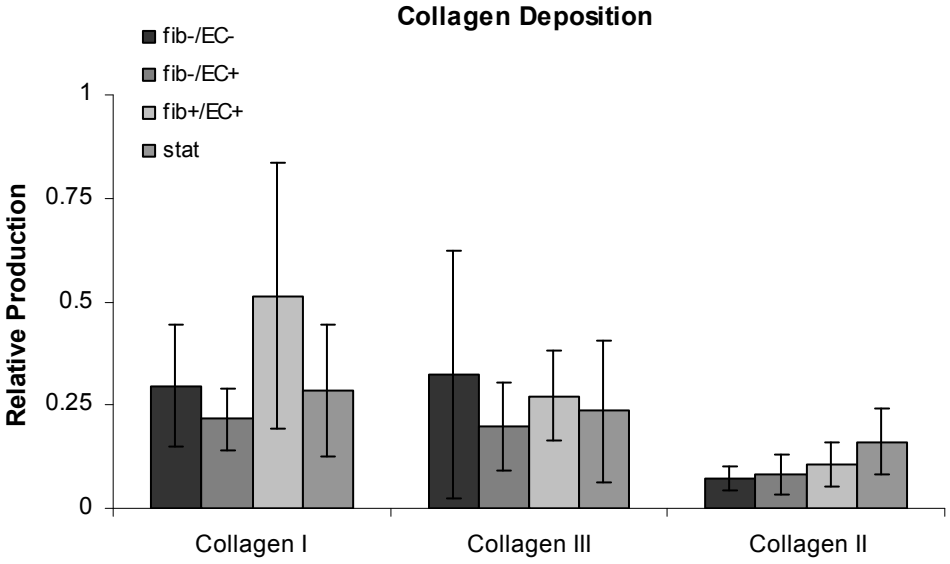

Figure 5.2: Collagen deposition by quantitative histological staining

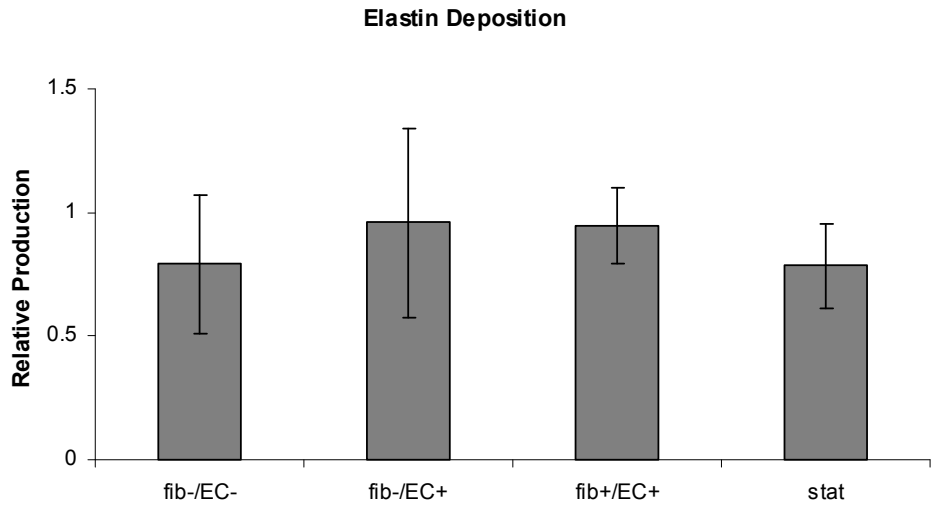

Figure 5.3: Elastin deposition by quantitative histological staining

Elastin was slightly elevated on average by the presence of ECs, but differences are not statistically significant. This is in agreement with previous experiments. Figure 5.4 shows the important differentiation markers for SMC development. Myocardin

directly regulates calponin h1 expression, and this trend is generally followed in the results. Contrary to experiments performed with mature SMCs, EC presence diminished both myocardin and calponin h1 expression. Standard deviations are too large to draw conclusions for SRF and elk-1, but elk-1 expression appears reduced with EC presence, also contrary to previous results. EC presence slightly elevated elk-1 expression, but was not statistically significant.

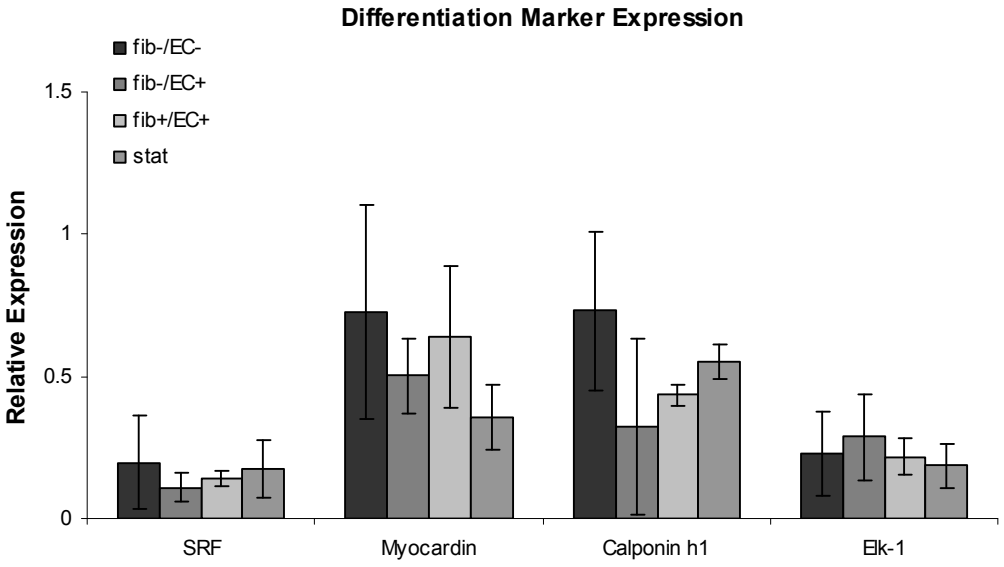

Figure 5.4: SMC differentiation marker expression by quantitative histological staining

Mesenchymal stem cells have the ability to differentiate into a variety of cell lines including SMCs, osteoblasts, chondrocytes, adipocytes and myocytes. Osteoblasts are present in bone tissue, chondrocytes are found in cartilage, adipocytes in fat tissue and myocytes in cardiac muscle. Each has different characteristic markers that can be

identified to test for preferential differentiation. For SMCs, osteoblasts, chondrocytes, adipocytes and myocytes, these markers are calponin h1, osteocalcein, collagen II, AFABP and skeletal cardiac α-actin (sk/cd α-actin), respectively. These markers (except collagen II and calponin h1) are shown in Figure 5.5. In general, dynamic conditioning and EC presence reduced expression of adipocyte, and myocyte phenotypes, in addition to chondrocytes as noted before.

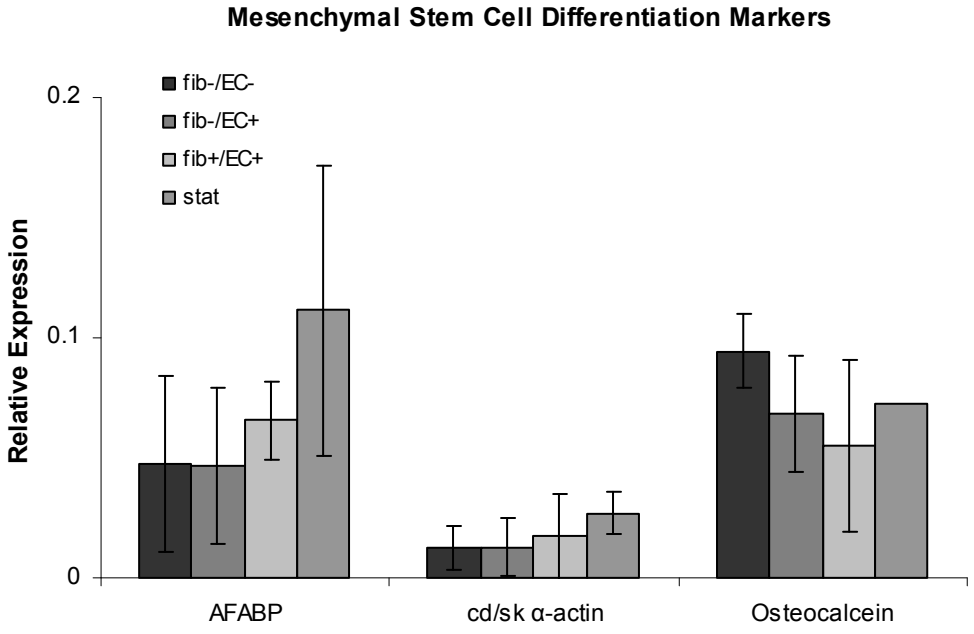

Figure 5.5: Mesenchymal stem cell differentiation markers from quantitative histological staining

To gain further insight into the SMC differentiation pathway via SRF, samples were stained for sp-1, SM α-actin, c-fos and c-jun. SM α-actin, like calponin h1, is a late term differentiation marker for SMCs. As noted before, pelk-1 competes with myocardin as an SRF binding partner and favors proliferation over differentiation.

Binding of pelk-1 results in c-fos expression. In addition, c-jun pairs with c-fos in this signaling pathway. Taken together, these results give more information into which pathway the SMCs are favoring and are presented in Figure 5.6. Binding partners c-jun and c-fos were overall enhanced in expression by EC presence. Sp-1 appeared elevated by EC presence, while SM α-actin was slightly reduced. Taken together, these results indicate that the presence of an endothelial layer inhibits the differentiation-favoring pathway, while favoring the proliferation pathway.

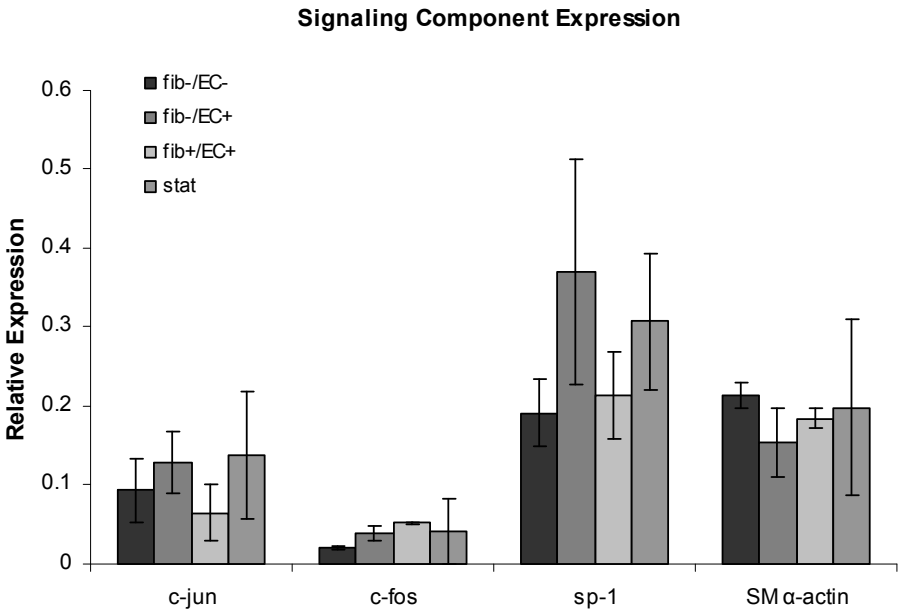

Figure 5.6: SMC differentiation pathway markers from quantitative histological staining

CHAPTER VI

MECHANICAL CONDITIONING AND EC MONOLAYER ON RASMCs

6.1 Introduction

This experiment seeks to address a potential issue from previous bioreactor experiments, namely the 3-dimensional EC configuration. A technique for applying an EC monolayer was developed to more closely mimic the vascular structure seen *in vivo*. Also, mature cell lines were used in an attempt to verify the results from previous experiments where a 3-dimensional EC scaffold was used. MSCs may react differently to EC presence than mature SMCs; therefore, the tubular structure must first be eliminated as a factor.

6.2 Experimental

A brief experimental will be presented here. For a more detailed description, see the relevant methods sections in Chapter II (Bioreactor III). The inner layer of the TEVGs was prepared with a BAEC (passage 9-12) monolayer at a density of $30x10^6$ cells/mL. A precursor solution of 0.1 g/mL PEGDA and 1μmol/mL ACRYL-PEG-RGDS and 10μL/mL acetophenone in HBS-TEOA was prepared, sterilized by filtration and used to resuspend the BAECs. The solution was then spread on a glass rod (4mm diameter) between two Teflon cylindrical molds in a monolayer form and dried under

sterile air. A plastic cylinder of diameter 7.4mm was then added to the cylindrical mold to enclose the EC layer. An equivalent PEGDA precursor solution with resuspended SMCs (passage 9-12, $2x10^6$ cells/mL) was then added to the cylindrical mold (~0.7mL/construct) and photopolymerized under longwave UV for 2 minutes. The resulting hydrogels were removed from their molds and briefly rinsed in PBS containing 1% PSA (10 U/mL penicillin, 10 g/L streptomycin, and 10 g/L amphotericin, Mediatech, Manassas). Constructs were then immersed in DMEM containing 10% BCS and 1% PSA and were cultured statically at 37 ºC/5% CO_2 for 3 days to ensure contamination did not occur. Media was changed every day until constructs were collected for mechanical conditioning.

This experiment was performed with three constructs run under dynamic mechanical conditioning and three constructs left under static conditions. Media was changed every 2-3 days to replenish nutrients, stabilize pH and prevent contamination. The system was run for a total period of 15 days. For the first 7 days, flow was slowly and systematically ramped from 60 Ml/min to a final flow rate of 360 Ml/min, yielding an average flow of 120 Ml/min per construct. Pulsation was introduced at day 4, and the average waveform was 65/40mmHg with ~160bpm when full flow was achieved on day 9. After 15 days, samples were collected from both dynamic and static constructs, which will be denoted as dyn+ and dyn- for results discussion. Samples were collected by cutting ring segments from each construct. Segments allocated for biochemical analysis were snap frozen in liquid N_2 and stored at -80°C until use. Sections designated for mechanical testing were rinsed in PBS and immediately tested to avoid any introducing

any physical changes to the samples. Histological sections were frozen in Tissue Tek (Sakura Finetek) media overnight at -20°C.

Histological stainings for calponin h1 and SRF were conducted to test for SMC phenotype and maturity. In addition, ECM markers collagen I and III were stained and analyzed. Biochemical analysis included DNA for determination of cell viability, total collagen, elastin and sGAG. Viability for the EC layer during the experimental run was verified by testing for nitrous oxide synthase (NOS) and von Willebrand factor (vWF), common EC markers (*88, 118*). In addition, a live/dead assay was performed to

6.3 Results and Discussion

Tensile mechanical testing yielded similar average values for both dyn+ and dyn- constructs. For the dyn+ constructs, the average modulus was 67.5 ± 2.1 kPa, while the dyn- construct average was 68.5 ± 4.7 kPa. Combining the elastic modulus values for the dynamic constructs with the applied average ΔP of 20mmHg in eq2 yields an average circumferential strain of ~8% experienced by SMCs during *in vitro* mechanical conditioning. In addition, eq3 yielded a mean wall shear stress of ~1 dyn/cm^2.

The staining for vWF appear in a localized fashion, indicating the EC luminal layer remained intact with minimal to no inter-layer migration of ECs. NOS in TEVGs has been shown to inhibit hyperplasia and maintain SMC homeostasis (*119*). Its presence here is desirable and expected in dynamic constructs. Figure 6.1 includes representative stainings for these markers. In addition, Figure 6.1 includes a fluorescent image of a live/dead assay as an indicator of cell viability. Figure 6.1 includes data from

24h post fabrication (A-C), 48h of high shear flow conditioning (D-F, I) and prolonged low shear flow conditioning (G,H). Image A is a brightfield image of the fabricated EC layer. Image B is a fluorescent image of a live/dead stain of the same layer and image C is a background fluorescent image for comparison to the live/dead image in B. Comparison of these two images indicates high cell viability and low cell loss. Images D-F are the same data after 48h of abrupt, high shear conditioning. Images G and H are histological stains for vWF and NOS, respectively after long exposure to low intensity shear conditioning. These images indicate success of the procedure used to form the monolayer of these TEVGs and long-term cell viability.

Calponin h1 is an indicator of SMC phenotype and is directly regulated by SRF (*48-50*). These were stained and counted for a semi-quantitative comparison. This information is included in Figure 6.2 along with ECM deposition immunostaining including collagen I, III and elastin. SRF expression was unchanged through dynamic conditioning, but calponin h1 expression was significantly enhanced in the dyn+ constructs. This indicates that *in vivo* dynamic conditioning enhances SMC maturity. ECM deposition of elastin was unchanged between dyn+ and dyn- constructs, whereas deposition of both collagen I and III was enhanced in dyn+ constructs. Stainings for ECM components also showed pericellularly localized deposition immediately surrounding the SMCs, which has been noted in similar work with PEGDA (*27, 88*).

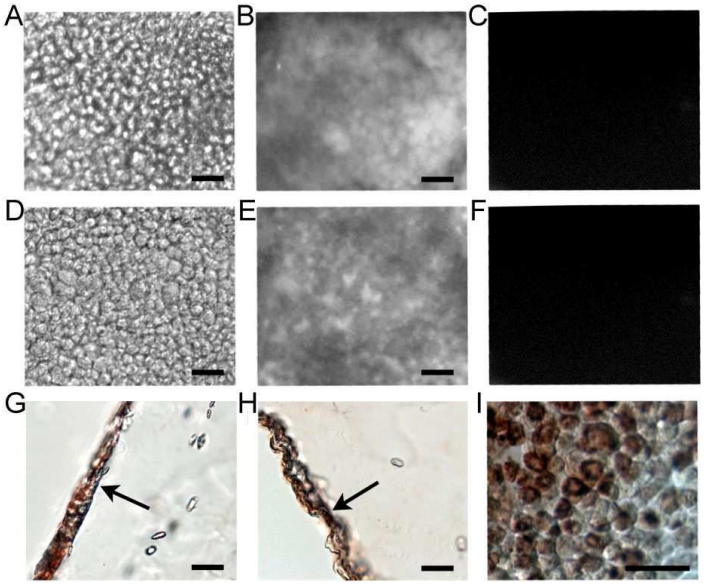

Figure 6.1: Dual-layer live/dead stainings. A-C) Images after 24h abrupt, high shear conditioning, A) Brightfield image of prepared EC monolayer, B) Fluorescent image of live/dead assay on EC layer, C) Background fluorescence for comparison to B. D-F) Images after 48h slow, low shear conditioning, D) Brightfield image of prepared EC monolayer, E) Fluorescent image of live/dead assay on EC layer, F) Background fluorescence for comparison to D. G) Histological staining for vWF after prolonged, low shear conditioning. H) Histological staining for NOS after prolonged, low shear conditioning. I) Histological staining for occludin after abrupt, high shear conditioning. Red coloration indicates a positive stain. Scale bars are 40 μm

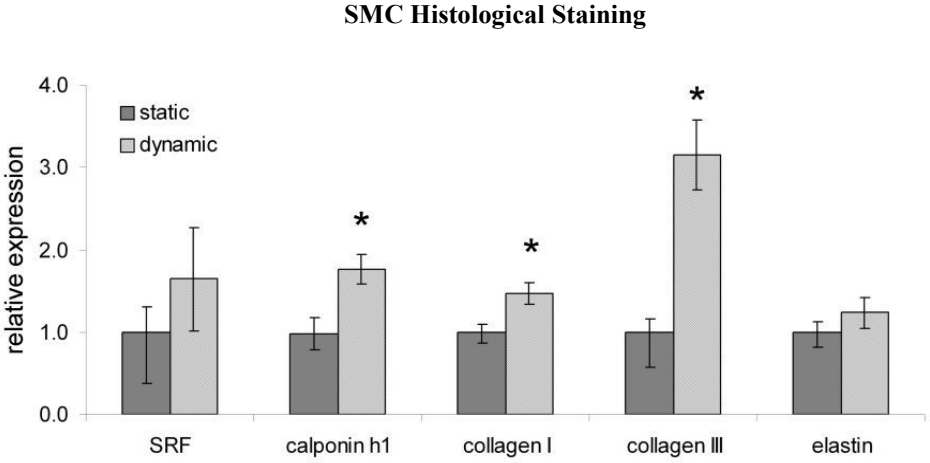

Figure 6.2: Semi-quantitative histological staining results for SMC phenotype markers and ECM deposition. *Significant different between dyn+ and dyn- constructs

Figure 6.3 shows the localized nature of ECM deposition of SMCs in the TEVGs.

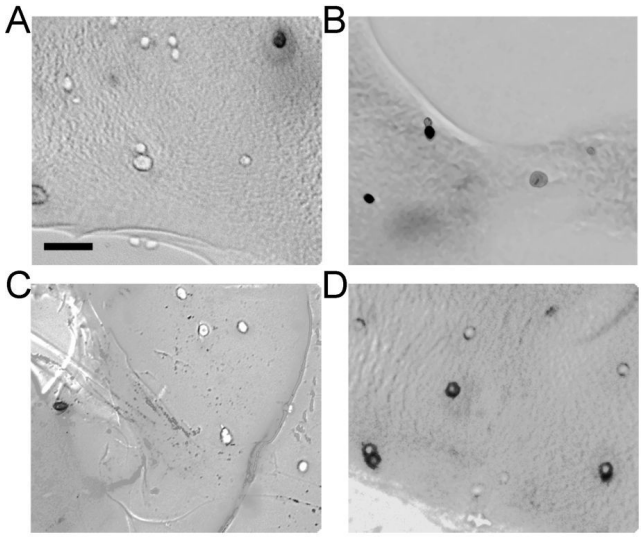

Figure 6.3: Histological stainings for SMCs. A,B) Calponin h1 in dyn- and dyn+ constructs, respectively. C,D) Collagen I in dyn- and dyn+ constructs, respectively. Positive stainings are black. Scale bar = 40μm

Biochemical analyses were performed to supplement the histological staining data for ECM deposition and are shown in Figure 6.4. Prior to analysis, the EC layer was removed from each construct so that all results could be directly applied to the SMC layer. DNA analysis yielded a cell density of ~$2x10^6$ cells/g, indicating strong cell viability during dynamic conditioning. Analysis of total collagen showed higher average values for dyn+ constructs, but these differences were not statistically significant. Results from the other analyses also were not statistically significant. The combined data show an influence of mechanical conditioning on SMC phenotype and behavior,

though more samples will be needed to minimize the standard deviations in the biochemical analyses.

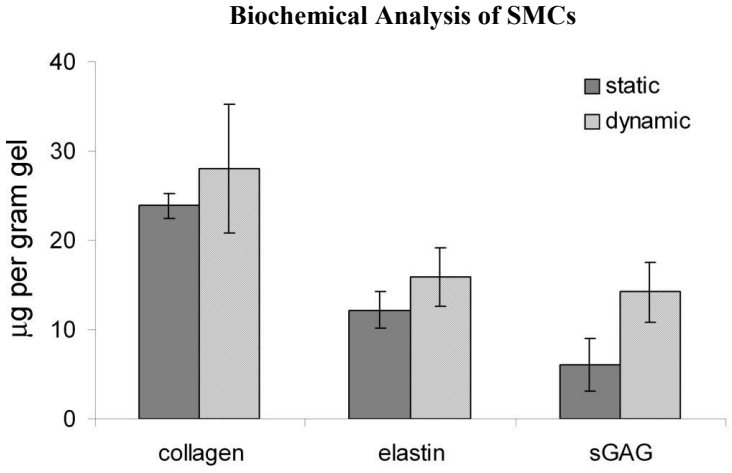

Figure 6.4: Biochemical analysis of SMCs for total collagen, elastin and sGAG. Differences were not statistically significant

A second experiment was conducted with the same setup as the first under which constructs were prepared and subjected to high shear conditions (~10 dyn/cm^2) over 2 days. Similar results for luminal layer viability were obtained with the additional expression of occludin, shown in Figure 6.1. Occludin regulates vascular wall permeability, associated with a quiescent EC phenotype (*120*).

CHAPTER VII

$PDMS_{star}$-PEG HYDROGELS

7.1 Introduction

Previous bioreactor experiments sought to investigate the individual and combined effects of cell-cell interactions and mechanical conditioning. Another important component for *in vitro* culture conditions for TEVGs is scaffold physical properties, including elastic modulus, water content and surface morphology, mesh size and degradation rate. PEGDA hydrogels have a relatively limited range on the extent of mechanical properties than can be achieved. Incorporation of PDMS into the PEG hydrogel network allows for a much wider control over scaffold physical properties, spanning both above and below those of native tissue. Novel $PDMS_{star}$ materials were developed by the Grunlan group for study in TEVGs. Incorporation of $PDMS_{star}$ into the hydrogel network allows for retention of the non-biofouling nature of pure PEG while giving systematic control over elastic modulus, water content and surface morphology (*70, 71, 73, 74*).

Preliminary studies by the Hahn and Grunlan groups (*72*) have shown significant control over scaffold modulus and differences in ECM deposition and differentiation marker expression on 10T1/2 mesenchymal stem cells. Changing PDMS content changed the cell phenotype that was enriched, suggesting optimization of the scaffold physical properties may allow for selective differentiation of mesenchymal stem cells

toward SMCs. Initial experiments were conducted with 6kDa PEG combined in 1:99, 5:95 and 10:90 weight ratios ($PDMS_{star}$:PEG) with 1.8kDa, 5kDa and 7kDa MW $PDMS_{star}$. This research seeks to expand the formulations tested in order to seek a method to fully optimize elastic modulus, water content and surface morphology. The property space being sampled was shown in Figure 1.9. This work utilizes the TEVG synthesis procedure developed during the bioreactor experiments to create cylindrical grafts.

7.2 Experimental

A brief experimental will be presented here. For a more detailed description, see the relevant methods sections in Chapter II. Formulations selected for synthesis were shown in Table 2.3, which is reproduced here. 10T1/2 mesenchymal stem cells at passage 21 were harvested and resuspended at a density of $3x10^6$ cells/mL in sterile-filtered precursor solutions according to Table 2.3 with an overall polymer concentration of 10% in HBS-TEOA with 1μmol/Ml ACRYL-PEG-RGDS. Precursor solutions (~0.8mL) were added to UV transparent cylindrical molds with Teflon bases. The molds had an outer diameter of 7.4mm with an inner diameter of 5mm. Solutions were then photopolymerized under longwave UV for a period of 5mins. The tri-layered hydrogels were removed from their molds and briefly rinsed in PBS containing 1% PSA. Constructs were then immersed in DMEM containing 10% BCS and 1% PSA and were

cultured statically at 37 ºC/5% CO_2 for a period of 21 days. Media was changed every two days until samples were harvested for analysis.

Table 2.3: Compositions of $PDMS_{star}$-PEGDA hydrogels used to study the effects of scaffold physical properties on SMC behavior. As an example of the ratios presented, 95:5 refers to an overall 10% polymer solution in HBS-TEOA, 95% being PEGDA and 5% being $PDMS_{star}$. For the last two combined formulations, the overall polymer concentration is again 10% in HBS-TEOA, half of which is the 3.4k formulation and half of which is the 6k formulation

PEGDA MW (kDa)	PDMSstarMA MW (kDa)	PEGDA:PDMSstarMA
3.4	0	100:0
	1.8	95:5
	1.8	80:20
	5	95:5
	7	99:1
	7	80:20
6	0	100:0
	5	90:10
	7	80:20
3.4,6	5	99:1, 80:20
	5	80:20, 80:20

For these formulations, solutions were prepared in equal amounts of the ratios shown, half of the 3.4k formulation and half of the 6k formulation

Constructs were cut into ring segments. End segments were discarded. Samples for biochemical analysis were snap frozen in liquid N_2 and stored at -80°C until use. Samples designated for histological analysis were frozen in Tissue Tek media at -20°C. Samples for mechanical conditioning were rinsed with PBS and immediately tested for elastic modulus. Quantitative histology was performed to examine ECM deposition and to test for 10T1/2 differentiation pathways. In addition, ECM deposition was analyzed via biochemical analysis. For simplicity in discussion, a condensed nomenclature will

be used. For example, 3.4 1.8/5 will refer to a hydrogel from 3.4kDa PEGDA and 1.8kDa $PDMS_{star}$ in a 95:5 ratio.

7.3 Results and Discussion

Final mechanical results are shown in Figure 7.1. The elastic modulus distribution did not yield expected results. As a group, the 3.4 kDa PEGDA hydrogels generally agree with previously seen trends. The 6 kDa PEGDA hydrogel formulations, however, trend higher than expected, and are not significantly different from the 3.4 kDa formulations. Therefore, the results analysis will focus on the 3.4 kDa formulations and relate observed trends to inorganic content.

Figure 7.2 shows the biochemical analysis of overall collagen content. In general, an increase in PDMS content increased overall collagen production. 3.4k 5/5, 3.4k 1.8/10 and 3.4k 7/20 have the highest overall collagen production and are significantly different from the other formulations. 3.4k 7/1, 3.4k 1.8/5 and 3.4k 1.8/20 showed similar collagen numbers and are significantly different from the pure 3.4k control.

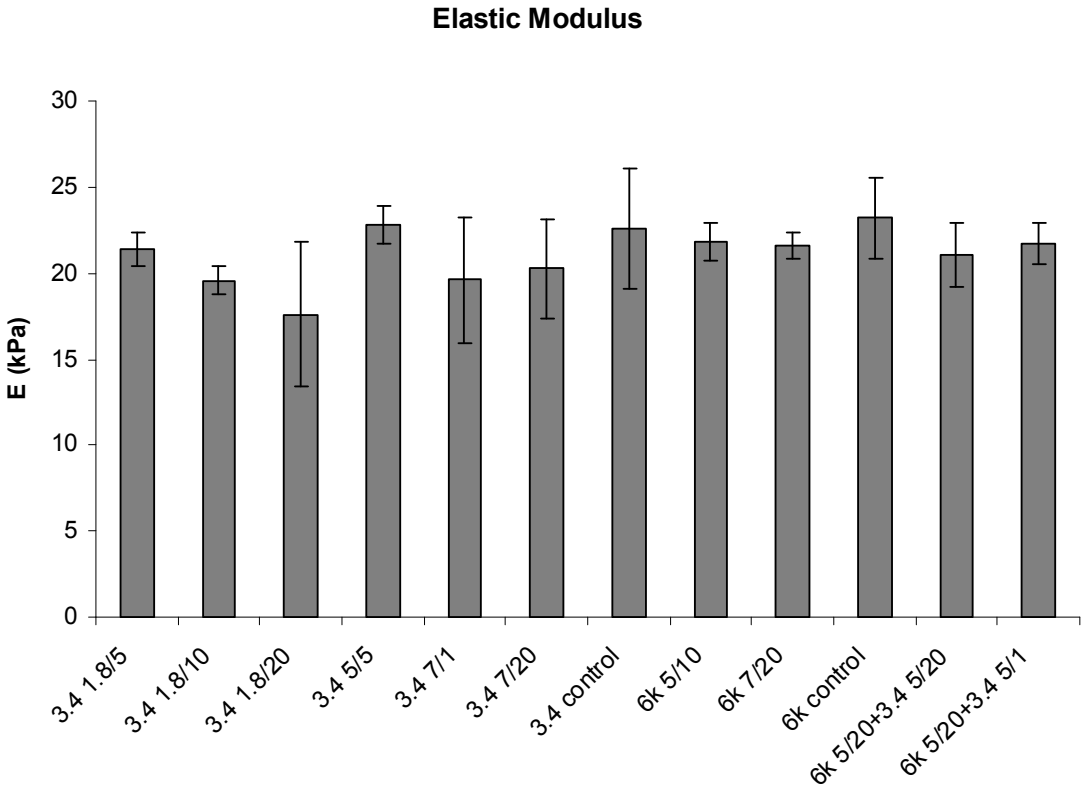

Figure 7.1: Mechanical data for $PDMS_{star}$-PEG co-hydrogels after experimental run

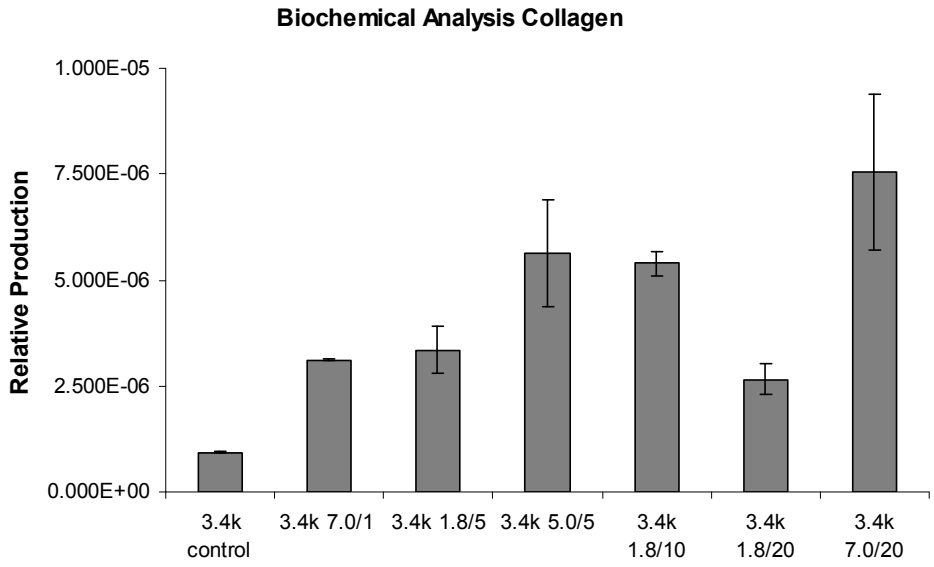

Figure 7.2: Total collagen production from biochemical analysis

Figure 7.3 shows the elastin production determined from the biochemical assay. In general, formulations did not show a significant difference in overall elastin production. 3.4k 7/1 was an exception, showing significant difference from the other formulations. 3.4k 7/20 exhibited a higher average than the other formulations, but could not be statistically justified. This could indicate higher MW PDMS content is beneficial for elastin production. This slightly contradicts preliminary measurements which showed overall reduction in elastin deposition with any PDMS presence (*72*). More work into the underlying signaling pathways would need to be performed to fully study these effects.

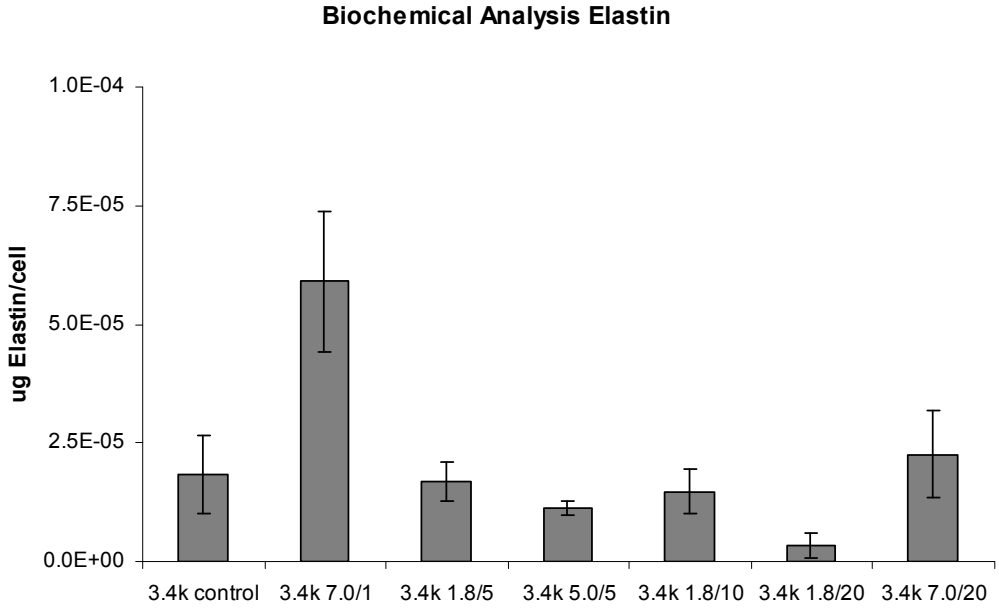

Figure 7.3: Elastin production from biochemical analysis

Figure 7.4 shows quantitative immunostaining results for collagen deposition. The general trends agree with the biochemical analysis. Increasing PDMS content appears to enhance collagen production. However, standard deviations are too large to

draw statistical conclusions about the data. Collagen I was enriched in the 3.4 1.8/5 formulation. For collagen II and III, the 20% PDMS content gels showed the highest levels in addition to the 0% control. These are general trends as standard deviations are too large to draw statistical conclusions.

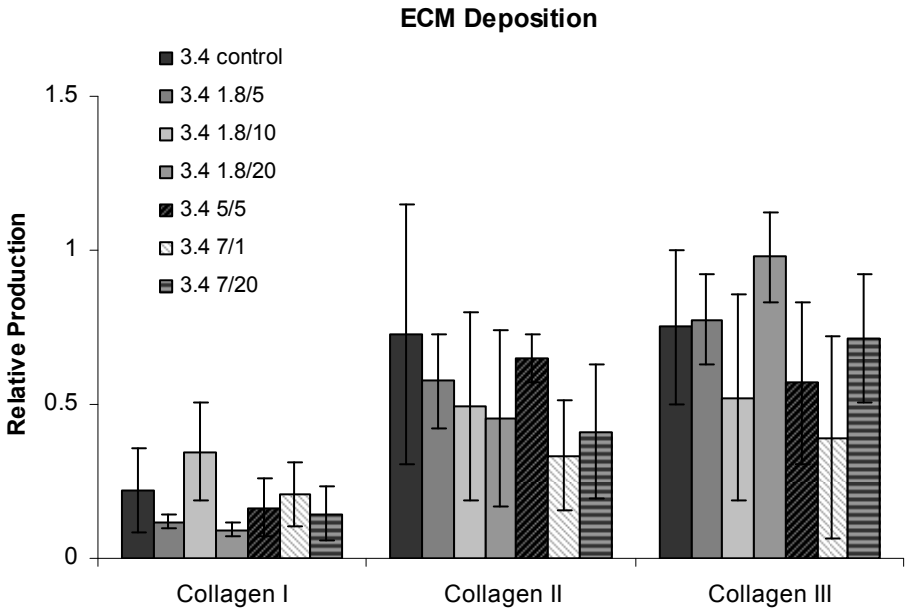

Figure 7.4: Collagen production from quantitative histological staining

Mesenchymal stem cells have the ability to differentiate into a variety of cell lines including SMCs, osteoblasts, chondrocytes, adipocytes and myocytes. Osteoblasts are present in bone tissue, chondrocytes are found in cartilage, adipocytes in fat tissue, and myocytes in cardiac muscle. Each has different characteristic markers that can be identified to test for preferential differentiation. For SMCs, osteoblasts, chondrocytes, adipocytes and myocytes, these markers are calponin h1, osteocalcein, collagen II,

AFABP and skeletal cardiac α-actin (sk/cd α-actin), respectively. These markers (except collagen II) are presented in Figures 7.5 and 7.6.

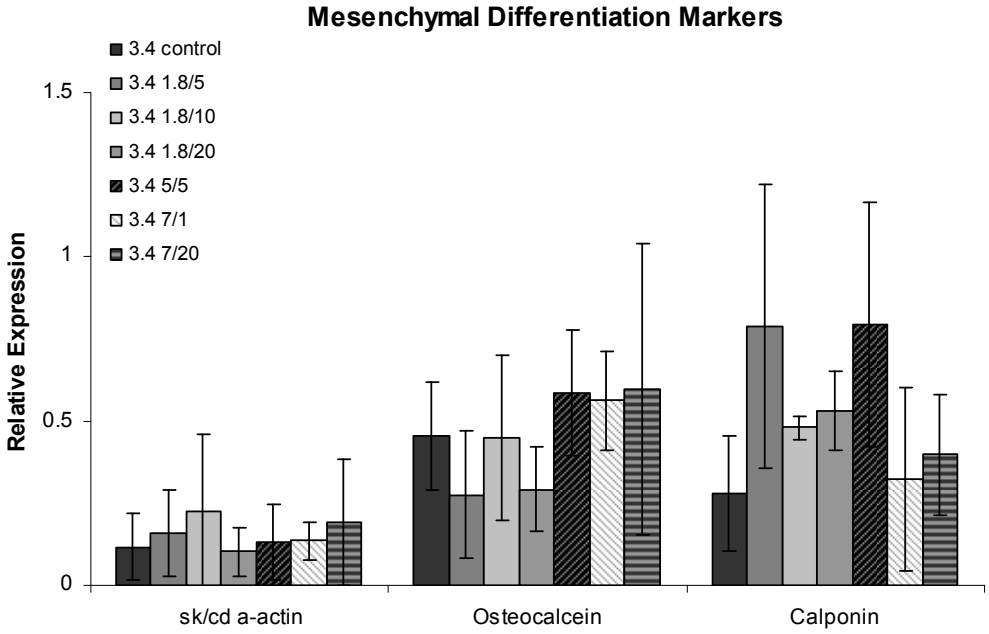

Figure 7.5: Differentiation markers for mesenchymal cell lines from quantitative histological staining

Standard deviations are too large to draw statistical conclusions. However, some general trends are apparent. Most important for TEVG implications are the 95:5 ratio formulations and their apparent enhanced expression of calponin h1. The results for this particular ratio are in agreement with previously observed results as shown in Figure 7.7 (*72*). Further analysis into the underlying signaling pathways responsible for calponin h1 upregulation needs to be performed to fully understand this apparent selectivity for SMCs.

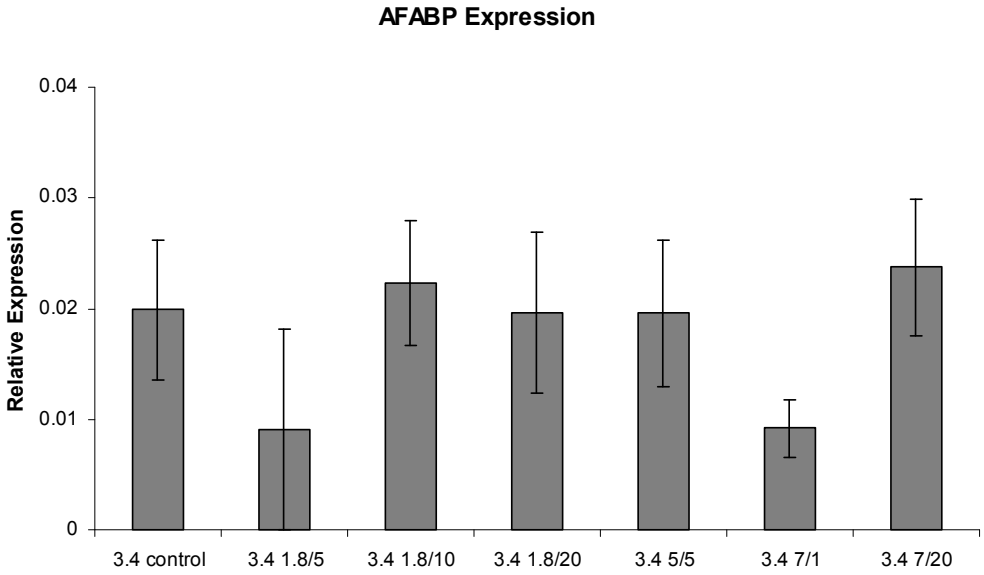

Figure 7.6: AFABP expression from quantitative histological staining

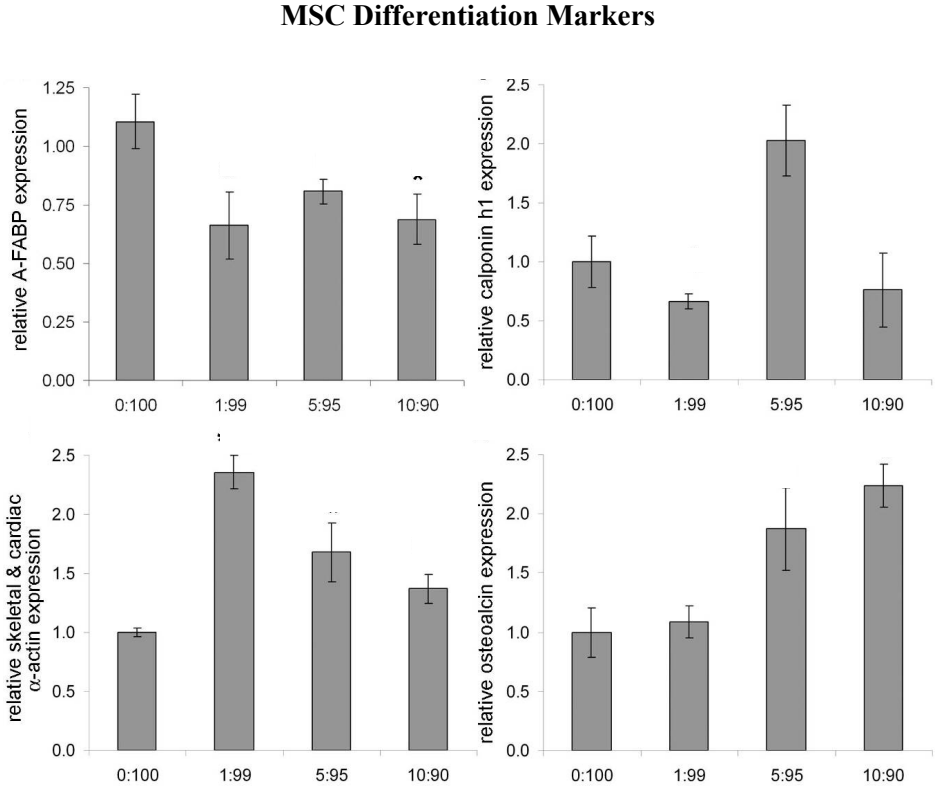

Figure 7.7: Mesenchymal cell differentiation markers from previous work (*72*)

For myocytes, the overall expression was low, with increasing PDMS content generally increasing expression, a trend opposite to the previous work with 6kDa PEG. The different PEG MW may also account for the differing trends. For osteocalcein, previous data showed increasing PDMS content enhanced expression. This general trend also appeared in this work, with lower MW PDMS showing greater enrichment. From the previous work, PDMS presence reduced expression of AFABP. This experiment isolates two formulations specifically which seem to limit AFABP expression, specifically 3.4 1.8/5 and 3.4 7/1, while higher PDMS content and the control gel showed higher presence of AFABP.

CHAPTER VIII

CONCLUSIONS AND FUTURE WORK

8.1 Vocal Fold Experiment

8.1.1 Conclusions

Current results indicate differences in the interactions between certain proteoglycans and PVFfs. The DS formulation was excluded from analysis because of its reduced elastic modulus. Elastic modulus has a significant effect on cell behavior, and for this formulation, could not be excluded as an experimental variable. Specifically, HA, CSC and HS produced equivalent amounts of collagen. However, CSC and HS produced a collagen I rich environment while HA was reduced in collagen I relative to CSC and HS. Relative to the other two formulations, HA was enriched in collagen III. In natural vocal fold tissue, generally the ECM is made up of equal parts of collagen I and III, with potential enrichment of collagen III. Relative ratios of collagen types have a significant impact on the mechanical properties of the tissue, with collagen III rich environments being associated with more elastic tissue. Preliminary analysis indicates a potential correlation between the ERK signaling transduction pathway, ECM production and SM α-actin expression, with enhanced ERK expression being associated with reduced SM α-actin deposition. CSC and HS also showed increased expression of SM α-actin, which is generally associated with vocal fold scarring. SM α-actin is

indicative of a transition from a fibroblast to a myofibroblast phenotype, which are present under tissue repair and scarring. It can be concluded that different GAGs do influence VFf behavior, but more work will need to be done to more thoroughly probe the extent of this influence and how they may be optimized.

8.2.2 Suggested Future Work

Suggested future work consists of an equivalent experiment which will include DS as a proteoglycan of interest. The results from this formulation could not be included here for discussion because of the differences in that gel's mechanical properties. In order to systematically study all components that control cell behavior, the different relevant factors need to be decoupled so that specific conclusions may be drawn. In addition, other components important in vocal fold tissue may be studied for any potential influence over cell behavior including fibronectin and fibrinogen. Further work, including RT-PCR studies and Western blotting should be performed to better understand the ERK and PKC transduction pathways and how they affect ECM production. RT-PCR can give a more in depth picture of the signaling pathways and how they are reacting to produce differences in ECM deposition and SM α-actin expression and how this might be prevented. Western blotting can support histological staining results and improve statistical conclusions via enhanced sample size.

8.2 Bioreactor Experiments

8.2.1 Conclusions

The initial bioreactor experiment utilized mature cells in a dual-layered configuration. Both an EC layer and a SMC layer were created. Cell migration between graft layers did not occur, allowing for conclusions from results obtained via histology, immunoblotting and gene expression to be applied to the medial SMC layer. Results from this experiment show a strong correlation between EC presence and mechanical conditioning on both SMC differentiation markers and ECM deposition. Results show that both components are independently important in ensuring a mature phenotype and maximizing elastin production. Collagen I deposition appeared reduced by the presence of ECs, so more work studying the underlying signaling pathways for collagen production need to be performed to prevent this in future TEVGs. Some limitations for this experiment hinder some areas of analysis. Sample size, while consistent with other similar experiments, proved small, yielding large standard deviations, making distinctions between results for some formulations impossible due to statistical significance. Also, the EC layer was synthesized as a 1mm thick 3-dimensional scaffold. This is in contrast to the monolayer structure typically seen in native vascular tissue. Future experiments may need to refine the luminal layer design to more closely mimic the natural EC monolayer.

The next experiment introduced the adventitial fibroblast layer with an EC layer, while still 3-dimensional in orientation, reduced to 0.5mm thick. Also, MSCs were utilized to investigate inter-cellular communication and mechanical conditioning affect the differentiation of progenitor cells. The quantitative histological staining presented here shows some results consistent with previous work with many major trends reversed. Like previous bioreactors, stainings showed localized deposition of matrix proteins. Also, migration of ECs did not occur in any significant amount. The magnitudes of standard deviations and small sample size have not allowed for statistical conclusions to be made, but general trends can be observed. EC presence appeared to reduce myocardin and calponin h1 expression. Since they are binding partners, the trends between reactors would be expected to match, which they do here. Contrary to previous results, EC presence under dynamic conditioning did not appear to reduce collagen I deposition. Mechanical conditioning and EC presence appear to be more important than fibroblast presence, but further tri-layered studies will need to be performed to verify this. Mesenchymal progenitor cells appear to react differently than mature SMCs to EC presence. This may be either a function of the cell type, or a difference in the 3-dimensional layout of the EC layer from the monolayer in natural tissue. Co-culture conditions will need to be investigated further to determine the optimal conditions for progenitor cell culture.

Given the reversal of trends seen with the MSC experiment, a method to synthesize an EC monolayer to more closely mimic natural vascular tissue was created. Also, a return to mature SMCs was made to discover any potential signaling differences

seen from the initial RASMC experiment given the difference in the EC layer construction. Preliminary studies indicate an influence of mechanical conditioning over both SMC phenotype and collagen production. One limitation early vascular graft work has suffered from is the lack of a suitable and stable endothelium under dynamic conditioning. The method presented here resulted in a stable EC layer with limited to no migration between graft layers. Experiments were conducted with abrupt, high shear conditioning as well as longer term, low shear conditioning, with both methods yielding a stable and intact EC layer. EC viability was also tested and confirmed through typical EC markers NOS, vWF and occluding.

Results from this experiment generally agreed with the initial mature cell line experiment. Dynamic conditioning enhanced ECM production and increased SRF expression, which also led to enhanced calponin h1 expression, indicating a more mature phenotype. These results are consistent with the initial study and show an ability to create a stable EC monolayer which closely mimics that of natural tissue. One limit of the current study, especially in terms of the biochemical analyses is sample size. The sample number used in this study is consistent with many similar studies, but yielded significant standard deviations, making comparisons between constructs difficult. Future studies will seek to increase samples for study to gain an enhanced understanding of the effects of mechanical conditioning.

8.2.2 Suggested Future Work

Further work can now be done by investigating the impact of an EC monolayer on MSCs in conjunction with mechanical conditioning. More experiments need to be conducted to determine the role EC presence plays in MSC differentiation and if it differs from the results seen with mature cell lines. Dynamic TEVG experiments may also begin to include investigation of changes in scaffold mechanical properties, specifically through the introduction of $PDMS_{star}$ into the hydrogel framework. The 95:5 ratio of PEG:$PDMS_{star}$ has been isolated to potentially enrich the SMC phenotype. Combining this formulation with EC presence and mechanical conditioning may further optimize the *in vitro* culture conditions. In addition, more experiments investigating the role of biochemical stimuli on SMCs may be performed. GAGs as well as other vascular components such as fibronectin and fibrinogen may have important implications in TEVG development. Once the most relevant biochemical stimuli are identified under static conditions, they too may be combined with mechanical conditioning and multi-layered grafts to attempt to improve SMC performance and differentiation. Future bioreactor experiments should attempt to include four samples per reactor rather than three. This will strengthen the statistics and make significant differences more apparent. Further experiments should be performed to more thoroughly analyze the impact of fibroblast presence and whether it is significant in SMC development and differentiation.

8.3 $PDMS_{star}$-PEG Hydrogels

8.3.1 Conclusions

Unexpected mechanical property results prevented the 6 kDa formulations from being included in this analysis. Some possible causes for the differences seen from previous measurements include incomplete crosslinking, excessive phase separation of PEG and PDMS in the precursor solutions and introduction of mechanical defects upon extraction from the cylindrical molds. Further experiments will need to be performed to attempt to systematically alter the modulus and its effects on cell behavior. This work, however, has successfully decoupled the effects of elastic modulus and the inorganic chemical environment.

Standard deviations and sample size limited the ability to draw statistical conclusions, but general trends could be observed. Overall, increasing PDMS content increased total collagen deposition. The most important implications for TEVGs are *in vitro* conditions that favor SMC differentiation. The 95:5 ratio formulations for PEG:$PDMS_{star}$ seem to enrich the SMC phenotype over other formulations. Relative to other formulations, the 95:5 ratio gels also showed diminished expression for chondrocyte, adipocyte, myocyte and osteoblast phenotypes. Results for osteocalcein also generally agreed with previous work showing with an increase in inorganic content enriching osteocalcein deposition. Increasing inorganic content also generally decreased expression of the chondrocyte phenotype while increasing the myocyte phenotype.

8.3.2 Suggested Future Work

Further experiments which include 6k formulations will need to be performed. To span a wider range of elastic moduli, and incorporate this as a separate design variable, other MWs of PEGDA may be included through 10 kDa. Formulations identified to enhance an SMC phenotype may be combined with other *in vitro* culture techniques, namely mechanical conditioning and cell co-culture, to attempt to optimize the development of TEVGs. This experiment consisted of three samples per formulation. To enhance statistical results, at least four samples per formulation should be studied. Histological analysis of differentiation markers can also be verified via qRT-PCR and Western blots. Western blots have an advantage over histological staining in that they include a larger sample size, enhancing statistical results. Utilizing qRT-PCR will give more insight into the underlying signaling pathways responsible for MSC differentiation. By optimizing and combining the *in vitro* culture conditions including scaffold properties, mechanical conditioning and multi-layered cell-cell interactions, 10T1/2 mesenchymal stem cells may be selectively driven to a mature SMC phenotype for use in TEVGs.

8.4 General Conclusions

This work has shown an influence of a variety of *in vitro* culture conditions on cell behavior. Identifying and optimizing each of these conditions and applying them to

tissue engineering studies may aid in the development of future vocal fold and TEVG experiments. Specifically, the factors identified include: biochemical stimuli in the synthetic scaffold, mechanical conditioning, cell-cell interactions, and scaffold physical properties.

REFERENCES

1. R. Langer, and J.P. Vacantie, *Science* **260**, 7 (1993).

2. E. H. Chung, Gilbert, M., Virdi, A.S., Sena, K., Sumner D.R. and Healy, K.E., *Journal of Biomedical Materials Research: Part A* **79A**, 12 (2006).

3. M. R. Lutolf, Weber F.E., Schomoekel, H.G., Schense, J.C., Kohler, T., Muller, R. and Hubbell, J.A., *Nature Biotechnology* **21**, 6 (2003).

4. M. M. Stevens, Marini, R.P., Schaefer, D., Aronson, J., Langer, R. and Shastri, V.P., *Proceedings of the National Academy of Sciences of the United States of America* **102**, 6 (2005).

5. A. P. Hollander, Dickinson, S.C., Sims, T.J., Brun, P., Cortivo, R., Kon, E., Marcacci, M., Zanasi, S., Borrione, A., De Luca, C., Paviesio, A., Soranzo, C. and Abatangelo, G., *Tissue Engineering* **12**, 11 (2006).

6. N. L'Heureux, Dusserre N, Marini A, Garrido S, Fuente L de la, and McAllister T, *Nature Clin Prac Card Med* **4**, 7 (July, 2007, 2007).

7. J. Viola, Lal, B. and Grad, O., *The Emergence of Tissue Engineering as a Research Field* (National Science Foundation, Arlington, VA, 2003).

8. E. S. Place, George, J.H., Williams, C.K. and Stevens, M.M., *Chemical Society Reviews* **38**, 13 (2008).

9. C. Hiemstra, Zhou, W., Zhong, Z.Y., Wouters, M. and Feijen, J., *Journal of the American Chemical Society* **129**, 9 (2007).

10. B. Lee. J., Y.H., Sohn, Y.S. and Jeong, B., *Biomacromolecules* **7**, 6 (2006).

11. Y. Murakami, Yokoyama, M. Okano, T., Nishida, H., Tomizawa, Y., Endo, M. and Kurosawa, H., *Journal of Biomedical Materials Research: Part A* **80A**, 7 (2007).

12. S. Nagahara, and T. Matsuda, *Polymer Gels and Networks* **4**, 17 (1996).

13. A. B. Pratt, Weber, F.E., Schmoekel R.M. and Hubbell, J.A., *Biotechnology and Bioengineering* **86**, 10 (2004).

14. C. Wang, Stewart R.J. and Kopecek, J., *Nature* **397**, 4 (1999).

15. N. Yamaguchi, Zhang, L., Chae, B.S., Palla, C.S., Furst, E.M. and Kiick, K.L., *Journal of the American Chemical Society* **129**, 2 (2007).

16. S. D. Gray, *Otolaryngologic Clinics of North America* **33**, 19 (2000).

17. H. E. Gunter, Harvard University (2003).

18. T. H. Hammond, Zhou, R., Hammond, E.H., Pawlak, A. and Gray, S.D., *Journal of Voice* **11**, 8 (1997).

19. X. Jia, Burdick, J.A., Kobler, J., Clifton, R.J., Rosowski, J.J., Zeitels, S.M. and Langer, R., *Macromolecules* **37**, 20 (2004).

20. J. E. Huber, Spievack, A., Ringel, R.L., Simmons-Byrd, A., and Badylak, S., *Annals of Otology, Rhinology & Laryngology* **112**, 6 (2003).

21. I. R. Titze, Hitchcock, R.W., Broadhead, K., Webb, K., Li, W., Gray, S.D. and Tresco, P.A., *Journal of Biomechanics* **37**, 9 (2004).

22. J. M. Chupa, Foster, A.M., Sumner, S.R., Madihally, S.V. and Matthew, H.W.T., *Biomaterials* **21**, 8 (2000).

23. S. Duflo, Thibeault, S.L, Wenhua, L.I., Shu, X.Z. and Prestwich, G.D., *Tissue Engineering* **12**, 8 (2006).

24. Y. Luo, Kobler, J.B., Zeitels, S.M and Langer, R., *Tissue Engineering* **12**, 10 (2006).

25. W. G. Gombotz WR, Horbett TA, and Hoffman AS, *J Biomed Mater Res* **25**, 16 (1991).

26. D. Benoit, Durney, AR, and KS Anseth, *Biomaterials* **28**, 12 (2007).

27. S. Bryant, and KS Anseth, *J Biomed Mater Res* **59**, 10 (Jan, 2002).

28. A. J. Bryant SJ, and Anseth KS, *Acta Biomateralia* **1**, 10 (2005).

29. S. L. Thibeault, Rousseau, B., Welham, N.V., Hirano, S. and Bless, D.M., *The Laryngoscope* **114**, 5 (2004).

30. P. D. Ward, Thibeault, S.L. and Gray, S.D., *Journal of Voice* **16**, 7 (2002).

31. X. Jia, Yeo, Y., Clifton, R.J., Jiao, T., Kohane, D.S., Kobler, J.B., Zeitels, S.M. and Langer, R., *Biomacromolecules* **7**, 9 (2006).

32. R. W. Chan, Gray, S.D. and Titze, I.R., *Otolaryngology-Head and Neck Surgery* **124**, 8 (2001).

33. *American Heart Association heart disease and stroke statistics-2005 update* (American Heart Association, Dallas, TX, 2005).

34. E. W. Schmedlen RH, Gobin AS, and West JL, *Clin Plast Surg* **30**, 11 (October 30, 2003).

35. W. Quinones-Baldrich, et al, *Ann Vasc Surg* **5**, 7 (1991, 1991).

36. S. JM, *Am Surg* **66**, 12 (2000, 2000).

37. F. Veith, et al, *J Vasc Surg* **3**, 11 (1986, 1986).

38. B. R. Seliktar D, Vito R, and Nerem R, *Ann Biomed Eng* **28**, 12 (2000).

39. A. Solan, Mitchell, S., Moses, M., and Niklason, L., *Tissue Engineering* **9**, 8 (2003).

40. B. Isenberg, and R Tranquillo, *Ann Biomed Eng* **31**, 3 (2003).

41. M. M. Hahn M, Wang E, Schmedlen R, and West J, *Ann Biomed Eng* **35**, 11 (2007).

42. R. Harvey, and N Rosenthal, *Heart Development*. (Academic Press, San Diego, 1999).

43. K. M. Ueba H, and Yaginuma T, *Arterioscler Thromb Vasc Biol* **18**, 5 (1997).

44. P. M. Garanich J, and Tarbell JM, *Am J Physiol Heart Circ Physiol* **288**, 9 (2005).

45. C. Williams, and TM Wick, *Ann Biomed Eng* **33**, 9 (2005).

46. C. T. Bryant SJ, Lee DA, Bader DL, and Anseth KS, *Ann Biomed Eng* **32**, 11 (2004).

47. T. J. Gray DS, and Chen CS, *J Biomed Mater Res Part A* **66A**, 10 (Sep 1, 2003).

48. L. X. Miano JM, and Fujiwara K, *Am J Physiol Cell Physiol* **292**, 12 (2007).

49. W. D.-Z. Wang Z, Hockemeyer D, McAnally J, Nordheim A, and Olson EN, *Nature Clin Prac Card Med* **428**, 5 (2004).

50. C. M. Miano J, Spencer J, and Misra R, *J Biol Chem* **275**, 9 (2000).

51. C. Weinberg, and E Bell, *Science* **231**, 4 (1986).

52. D. Swartz, et al, *Am J Physiol Heart Circ Physiol* **288**, 10 (2005).

53. T. Girton, et al, *J Biomech Eng* **122**, 8 (2000).

54. T. Shin'oka, et al, *N Engl J Med* **344**, 2 (2001).

55. P. Reusch, and H Wagdy, *Circulation Research* **79**, 8 (1996).

56. K. Birukov, and V Shirinsky, *Mol Cell Biochem* **144**, 9 (1995).

57. T. Kulik, and S Alvarado, *J Cell Physiol* **157**, 10 (1993).

58. M. Chiquet, and M Matthisson, *Biochem Cell Biol* **74**, 8 (1996).

59. D. N. Smith JD, Willis AI, Sumpio BE, and Zilla P, *Endothelium* **8**, 8 (2001).

60. C. O'Callaghan, and B Williams, *Hypertension* **36**, 6 (2000).

61. S. S. Engler AJ, Sweeney HL, and Discher DE, *Cell* **126**, 13 (Aug 25, 2006).

62. W. D.-Z. Wang Z, Pipes T, and Olson EN, *Proceedings of the National Academy of Sciences* **100**, 6 (Jun 10, 2003).

63. L. P. Riha GM, Lumsden AB, Yao Q, and Chen C, *Tissue Engineering* **11**, 19 (2005).

64. H. S. Kadner A, Zund G, Eid K, Maurus C, Melnitchouk S, Grunenfelder J, and Turina MI, *Eur J Cardiothorac Surg* **21**, (2002).

65. E. Lavik, and R Langer, *Appl Microbiol Biotechnol* **65**, (2004).

66. M. T. Hamilton DW, and Vorp DA, *Tissue Engineering* **10**, (2004).

67. G. N. Gojo S, Takeda Y, Mori T, Abe H, Kyo S, Hata J and Umezawa A, *Exp Cell Res* **288**, (2003).

68. M. A. Davani S, Mersin N, Royer B, Kantelip B, Herve P, Etievent JP and Kantelip JP, *Circulation* **108(Suppl 1)**, (2003).

69. K. C. Ringe J, Burmester GR and Sittinger M, *Naturwissenschaften* **89**, (2002).

70. C. S. G. Gudipati, C.M., Johnson, J.A., Prayongpan, P., Wooley, K.L., *Journal of Polymer Science Part A: Polymer Chemistry* **42**, 16 (2004).

71. M. A. L. Grunlan, N.S., Mansfeld, F., Kus, E., Finlay, J.A., Callow, M.E., Weber, W.P., *Journal of Polymer Science Part A: Polymer Chemistry* **44**, 16 (2006).

72. M.A. Grunlan, M.S. Hahn, M, National Institutes of Health Grant Proposal (Texas A&M University, College Station, TX, 2008).

73. R. Murthy, Cox, C.D., Hahn, M. and Grunlan, M.A., *Biomacromolecules* **8**, 9 (2007).

74. G. Cai, and Weber, W.P., *Polymer* **45**, 8 (2004).

75. T. L. Hahn M, Moon J, Rowland M, Ruffino K, and West J, *Biomaterials* **27**, 6 (2006).

76. K. R. Regan, Hou, Y., Hahns, M.S., Liao, H. and Grunlan, M.A., *PMSE Preprints (Amer. Chem. Soc., Div. Poly. Mater. Sci. Eng)* **96**, 2 (2007).

77. Y. Hou, Regan, K.R., Schoener, C.A., Hahn, M.S. and Grunlan, M.A., *POLY Preprints (Amer. Chem. Soc., Div. Poly. Chem.* **48**, 2 (2007).

78. A. Dudley, Gilbert, R.E., Thomas, D., Cox, A., Price, J.T., Best, J. et al, *Biochemical and Biophysical Research Communications* **310**, 8 (2003).

79. J. P. Eiserich, Baldus, S., Brennan, M-L, Ma, W., Zhang, C., Tousson, A., et al, *Science* **296**, 4 (2002).

80. N. Marczin, Papapetropoulos, A. and Catravas, J.D., *American Journal of Physiology-Heart and Circulatory Physiology* **265**, 5 (1993).

81. C. Pross, Farooq, M.M., Lane, J.S., Angle, N., Tomono, C.K., Xavier A.E., Freischlag, J.A., Collins, A.E., Law, R.E. and Gelabert, H.A., *Journal of Vascular Surgery* **35**, 7 (2002).

82. G. Gabbiani, *Annals of the New York Academy of Sciences* **488**, 3 (2006).

83. D. Gordon, Mohai, L.G. and Schwartz, S.M., *Circulation Research* **59**, 11 (1986).

84. H. Hao, Gabbiani, G. and Bochaton-Piallat, M.L., *Arterioscler Thromb Vasc Biol* **23**, 11 (2003).

85. R. J. Hamill, Vann, J.M. and Proctor, R.A., *Infection and Immunity* **54**, 4 (1986).

86. J. B. Sanctis, Arciniegas, E. and Bianco, N.E., *Cellular Immunology* **227**, 11 (2004).

87. G. a. M. Folcoand, R.C., *Pharmacological Reviews* **58**, 14 (2006).

88. Bulick. A.S., Munoz-Pinto, D.J., Qu, X., Mani, M., Christancho, D., Urban, M. and Hahn, M.S., *Tissue Engineering: Part A* **15**, 11 (2009).

89. A. I. Caplan, *Orthopaedic Research* **9**, 10 (1991).

90. H. a. C. Ohgushi, A.I., *Journal of Biomedical Materials Research* **48**, 16 (1999).

91. B. C. Heng, Cao, T. and Lee, E.H., *Stem Cells* **22**, 17 (2004).

92. W. M. Jackson, Aragon, A.B., Djouad, F., Song, Y., Koehler, S.M., Nesti, L.J. and Tuan, R.S., *Journal of Tissue Engineering and Regenerative Medicine* **3**, 10 (2009).

93. W. C. Nobuya U, Jenkins SL, Wentworth RA, Ding X-Y, Lu C, et al, *Am J Physiol Heart Circ Physiol* **276**, 9 (1999).

94. U. A. Stock, Vacanti, J.P., *Tissue Engineering* **7**, 7 (2001).

95. M. Hiles, Badylak, S., Lantz, G., Kokini, K., Geddes, L., and Morff, R., *Journal of Biomedical Materials Research* **29**, 9 (1995).

96. C. Johnson, How, T., Scraggs, M., West, C., and Burns, J., *Forensic Science International* **109**, 14 (2000).

97. J. a. G. Posey, L., *Cardiovascular Research* **11**, 6 (1973).

98. L. Brossollet, *International Journal of Artificial Organs* **15**, 6 (1992).

99. M. S. Hahn, Teply, B.A., Stevens, M.M., Zeitels, S.M. and Langer, R., *Biomaterials* **27**, 6 (2006).

100. J. Long, and Tranquillo, R., *Matrix Biology* **22**, 12 (2003).

101. A. B. Hummon, Lim, S.R., Difilippantonio, M.J. and Ried, T., *Biotechniques* **42**, 6 (2007).

102. S. D. Gray, Titze, I.R. and Hammon, A.F., *The Annals of Otology, Rhinology and Laryngology* **109**, 9 (2000).

103. A. S. Pawlak, Hammond, T., Hammond, E. and Gray, S.D., *The Annals of Otology, Rhinology and Laryngology* **105**, 6 (1996).

104. J. K. a. T. Hansen, S.L., *Journal of Voice* **20**, 11 (2005).

105. M. Culty, Miyake, K., Kincade, P.W., et al, *Journal of Cell Biology* **111**, 10 (1990).

106. C. B. Underhill, Green, S.J., Comogio, P.M. and Tarone, G., *Immunology Today* **262**, 5 (1987).

107. P. Herrlich, Zoller, M., Pals, S.T. and Ponta, H., *Immunology Today* **14**, 5 (1993).

108. R. van der Voort, Taher, E.I., Vera, J.M., Spaargaren, M., Prevo, R., Smit, L., Guido, D., Hartmann, G., Gherardi, E. and Pals, S.T., *Journal of Biological Chemistry* **274**, 8 (1999).

109. T. Fujimoto, Kawashima, H., Tanaka, T., Hirose, M., Toyama-Sorimachi, N., Matsuzawa, Y. and Miyasaka, M., *International Immunology* **13**, 8 (2001).

110. K. a. Y. Kitaya, T., *Journal of Leukocyte Biology* **85**, 10 (2009).

111. H. Ponta, Sherman, L. and Herrlich, P.A., *Nature Reviews Molecular Cell Biology* **4**, 13 (2003).

112. J. Entwistel, Hall, C.L. and Turley, E.A., *Journal of Cellular Biomechanics* **61**, 9 (1996).

113. K. B. Keys, Andreopoulos, F.M. and Peppas, N.A., *Macromolecules* **31**, 8 (1998).

114. E. M. Culav, Clark, C.H. and Maerrilees, M.J., *Physical Therapy* **79**, 12 (1999).

115. K. A. Costa, Sumpio. B.E. and Cerreta, J.M., *The FASEB Journal* **5**, (1991).

116. B. Kim, Nikolovski, J., Bonadio, J. and Mooney, Dr., *Nature Biotechnology* **17**, 5 (1999).

117. K. K. Hirschi, Rohovsky, S.A. and D'Amore, P.A., *Journal of Cell Biology* **141**, 10 (1998).

118. J. Elisseeff, Puleo, C., Yang, F. and Sharma, B., *Orthodontics & Craniofacial Research* **8**, 12 (2005).

119. N. E. Hastings, Simmers, M.B., McDonald, O.G., Wamhoff, B.R. and Blackman, B.R., *Am J Physiol Cell Physiol* **293**, 10 (2007).

120. T. Korff, Kimmina, S., Martiny-Baron, G. and Augustin, H.G., *The FASEB Journal* **15**, 9 (2001).

VITA

Name:	Allen Bulick
Address:	Department of Chemical Engineering c/o Dr. Mariah Hahn Texas A&M University College Station, TX 77843-3122
Email:	abulick@neo.tamu.edu
Education:	B.S., Texas A&M University, 2005 Ph.D., Texas A&M University, 2009